



AMS

American Meteorological Society

Supplemental Material

Journal of Hydrometeorology

Verification of Land–Atmosphere Coupling in Forecast Models, Reanalyses, and Land Surface Models Using Flux Site Observations

<https://doi.org/10.1175/JHM-D-17-0152.s1>

[© Copyright 2018 American Meteorological Society](#)

Permission to use figures, tables, and brief excerpts from this work in scientific and educational works is hereby granted provided that the source is acknowledged. Any use of material in this work that is determined to be “fair use” under Section 107 of the U.S. Copyright Act or that satisfies the conditions specified in Section 108 of the U.S. Copyright Act (17 USC §108) does not require the AMS’s permission. Republication, systematic reproduction, posting in electronic form, such as on a website or in a searchable database, or other uses of this material, except as exempted by the above statement, requires written permission or a license from the AMS. All AMS journals and monograph publications are registered with the Copyright Clearance Center (<http://www.copyright.com>). Questions about permission to use materials for which AMS holds the copyright can also be directed to the AMS Permissions Officer at permissions@ametsoc.org. Additional details are provided in the AMS Copyright Policy statement, available on the AMS website (<http://www.ametsoc.org/CopyrightInformation>).

Supplemental Information – Contents

	Page(s)
Table S1: Information on all FLUXNET2015 sites	1-5
Table S2: Information on gridded observed precipitation data sets	6
Fig. S1: Scatter diagram of MERRA products precipitation compared to FLUXNET2015 observations	7
Figs. S2-S14: Scatter diagrams for the annual mean values of variables from the models compared to FLUXNET2015 observations	8-20
Figs. S15-S24: Scatter diagrams for the magnitude of the annual cycle of variables from the models compared to FLUXNET2015 observations	21-30
Figs. S25-S34: Scatter diagrams for the phase of the annual cycle of variables from the models compared to FLUXNET2015 observations	31-40
References for Table entries	41-45

Table S1: Information for the FLUXNET2015 sites used in this study.

	ID	Longitude	Latitude	Years		Reference
1	AR-SLu	-66.4598	-33.4648	2009-2011	3y	fluxnet.fluxdata.org
2	AR-Vir	-56.1886	-28.2395	2009-2012	4y	fluxnet.fluxdata.org
3	AT-Neu	11.3175	47.1167	2002-2012	11y	Stoy et al. 2013
4	AU-Ade	131.1178	-13.0769	2007-2009	3y	Beringer et al. 2016
5	AU-ASM	133.249	-22.283	2010-2013	4y	Beringer et al. 2016
6	AU-Cpr	140.5891	-34.0021	2010-2014	5y	Beringer et al. 2016
7	AU-Cum	150.7225	-33.6133	2012-2014	3y	Beringer et al. 2016
8	AU-DaP	131.3181	-14.0633	2007-2013	7y	Beringer et al. 2016
9	AU-DaS	131.3881	-14.1593	2008-2014	7y	Jamali et al. 2011
10	AU-Dry	132.3706	-15.2588	2008-2014	7y	Beringer et al. 2016
11	AU-Emr	148.4746	-23.8587	2011-2013	3y	Beringer et al. 2016
12	AU-Fog	131.3072	-12.5452	2006-2008	3y	Beringer et al. 2016
13	AU-Gin	115.7138	-31.3764	2011-2014	4y	Beringer et al. 2016
14	AU-GWW	120.6541	-30.1913	2013-2014	2y	Beringer et al. 2016
15	AU-How	131.1523	-12.4943	2001-2014	14y	Beringer et al. 2016
16	AU-Lox	140.6551	-34.4704	2008-2009	2y	Beringer et al. 2016
17	AU-RDF	132.4776	-14.5636	2011-2013	3y	Beringer et al. 2016
18	AU-Rig	145.5759	-36.6499	2011-2014	4y	Beringer et al. 2016
19	AU-Rob	145.6301	-17.1175	2014-2014	1y	Beringer et al. 2016
20	AU-Stp	133.3502	-17.1507	2008-2014	7y	Beringer et al. 2016
21	AU-TTE	133.64	-22.287	2012-2013	2y	Beringer et al. 2016
22	AU-Tum	148.1517	-35.6566	2001-2014	14y	Beringer et al. 2016
23	AU-Wac	145.1878	-37.4259	2005-2008	4y	Beringer et al. 2016
24	AU-Whr	145.0294	-36.6732	2011-2014	4y	Beringer et al. 2016
25	AU-Wom	144.0944	-37.4222	2010-2012	3y	Fest et al. 2017
26	AU-Ync	146.2907	-34.9893	2012-2014	3y	Beringer et al. 2016
27	BE-Bra	4.5206	51.3092	1996-2014	19y	Stoy et al. 2013
28	BE-Lon	4.7461	50.5516	2004-2014	11y	Moureaux et al. 2006
29	BE-Vie	5.9981	50.3051	1996-2014	19y	Aubinet et al. 2001
30	BR-Sa3	-54.9714	-3.018	2000-2004	5y	doi:10.17190/AMF/1245995
31	CA-Man	-98.4808	55.8796	1994-2008	15y	doi:10.17190/AMF/1245997
32	CA-NS1	-98.4839	55.8792	2001-2005	5y	doi:10.17190/AMF/1245998
33	CA-NS2	-98.5247	55.9058	2001-2005	5y	doi:10.17190/AMF/1245999
34	CA-NS3	-98.3822	55.9117	2001-2005	5y	doi:10.17190/AMF/1246000
35	CA-NS4	-98.3822	55.9117	2002-2005	4y	doi:10.17190/AMF/1246001
36	CA-NS5	-98.485	55.8631	2001-2005	5y	doi:10.17190/AMF/1246002
37	CA-NS6	-98.9644	55.9167	2001-2005	5y	doi:10.17190/AMF/1246003
38	CA-NS7	-99.9483	56.6358	2002-2005	4y	doi:10.17190/AMF/1246004

	ID	Longitude	Latitude	Years		Reference
39	CA-Qfo	-74.3421	49.6925	2003-2010	8y	doi:10.17190/AMF/1246829
40	CA-SF1	-105.8176	54.485	2003-2006	4y	doi:10.17190/AMF/1246006
41	CA-SF2	-105.8775	54.2539	2001-2005	5y	doi:10.17190/AMF/1246007
42	CA-SF3	-106.0053	54.0916	2001-2006	6y	doi:10.17190/AMF/1246008
43	CH-Cha	8.4104	47.2102	2005-2014	10y	Merbold et al. 2014
44	CH-Dav	9.8559	46.8153	1997-2014	18y	fluxnet.fluxdata.org
45	CH-Fru	8.5378	47.1158	2005-2014	10y	Imer et al. 2013
46	CH-Lae	8.365	47.4781	2004-2014	11y	Heim et al. 2008
47	CH-Oe1	7.7319	47.2858	2002-2008	7y	Ammann et al. 2007
48	CH-Oe2	7.7343	47.2863	2004-2014	11y	Dietiker et al., 2010
49	CN-Cha	128.0958	42.4025	2003-2005	3y	fluxnet.fluxdata.org
50	CN-Cng	123.5092	44.5934	2007-2010	4y	fluxnet.fluxdata.org
51	CN-Dan	91.0664	30.4978	2004-2005	2y	fluxnet.fluxdata.org
52	CN-Din	112.5361	23.1733	2003-2005	3y	fluxnet.fluxdata.org
53	CN-Du2	116.2836	42.0467	2006-2008	3y	Stoy et al. 2013
54	CN-Ha2	101.3269	37.6086	2003-2005	3y	fluxnet.fluxdata.org
55	CN-HaM	101.18	37.37	2002-2004	3y	Li et al. 2013
56	CN-Qia	115.0581	26.7414	2003-2005	3y	fluxnet.fluxdata.org
57	CN-Sw2	111.8971	41.7902	2010-2012	3y	fluxnet.fluxdata.org
58	CZ-BK1	18.5369	49.5021	2004-2008	5y	Dařenova et al. 2016
59	CZ-BK2	18.5429	49.4944	2004-2006	3y	Dařenova et al. 2017
60	CZ-wet	14.7704	49.0247	2006-2014	9y	Stoy et al. 2013
61	DE-Akm	13.6834	53.8662	2009-2014	6y	fluxnet.fluxdata.org
62	DE-Geb	10.9143	51.1001	2001-2014	14y	Revill et al. 2013
63	DE-Gri	13.5125	50.9495	2004-2014	11y	Stoy et al. 2013
64	DE-Hai	10.453	51.0792	2000-2012	13y	Knohl et al. 2003
65	DE-Kli	13.5225	50.8929	2004-2014	11y	Revill et al. 2013
66	DE-Lkb	13.3047	49.0996	2009-2013	5y	fluxnet.fluxdata.org
67	DE-Obe	13.7196	50.7836	2008-2014	7y	Jung et al. 2009
68	DE-RuR	6.3041	50.6219	2011-2014	4y	Borchard et al. 2015
69	DE-RuS	6.4472	50.8659	2011-2014	4y	Schmidt et al. 2012
70	DE-Seh	6.4497	50.8706	2007-2010	4y	fluxnet.fluxdata.org
71	DE-SfN	11.3275	47.8064	2012-2014	3y	fluxnet.fluxdata.org
72	DE-Spw	14.0337	51.8923	2010-2014	5y	fluxnet.fluxdata.org
73	DE-Tha	13.5669	50.9636	1996-2014	19y	Bernhofer et al. 2003
74	DK-Fou	9.5872	56.4842	2005-2005	1y	Stoy et al. 2013
75	DK-NuF	-51.3861	64.1308	2008-2014	7y	Westergaard-Nielsen et al. 2013
76	DK-Sor	11.6446	55.4859	1996-2014	19y	Stoy et al. 2013
77	DK-ZaF	-20.5545	74.4814	2008-2011	4y	Soegaard & Nordstroem 1999

ID	Longitude	Latitude	Years	Reference
78	DK-ZaH	-20.5503	74.4732	2000-2014 15y Lund et al. 2012
79	ES-LgS	-2.9658	37.0979	2007-2009 3y fluxnet.fluxdata.org
80	ES-Ln2	-3.4758	36.9695	2009-2009 1y fluxnet.fluxdata.org
81	FI-Hyy	24.295	61.8475	1996-2014 19y Suni et al. 2003
82	FI-Jok	23.5135	60.8986	2000-2003 4y Reichstein et al. 2005
83	FI-Lom	24.2092	67.9972	2007-2009 3y fluxnet.fluxdata.org
84	FI-Sod	26.6378	67.3619	2001-2014 14y Stoy et al. 2013
85	FR-Fon	2.7801	48.4764	2005-2014 10y Bazot et al. 2013
86	FR-Gri	1.9519	48.8442	2004-2013 10y Loubet et al. 2011
87	FR-LBr	-0.7693	44.7171	1996-2008 13y Stoy et al. 2013
88	FR-Pue	3.5958	43.7414	2000-2014 15y Rambal et al. 2004
89	GF-Guy	-52.9249	5.2788	2004-2014 11y Bonal et al. 2008
90	IT-BCi	14.9574	40.5238	2004-2014 11y Reichstein et al. 2003
91	IT-CA1	12.0266	42.3804	2011-2014 4y fluxnet.fluxdata.org
92	IT-CA2	12.026	42.3772	2011-2014 4y fluxnet.fluxdata.org
93	IT-CA3	12.0222	42.38	2011-2014 4y fluxnet.fluxdata.org
94	IT-Col	13.5881	41.8494	1996-2014 19y Stoy et al. 2013
95	IT-Cp2	12.3573	41.7043	2012-2014 3y fluxnet.fluxdata.org
96	IT-Cpz	12.3761	41.7052	1997-2009 13y Wei et al. 2014
97	IT-Isp	8.6336	45.8126	2013-2014 2y fluxnet.fluxdata.org
98	IT-La2	11.2853	45.9542	2000-2002 3y fluxnet.fluxdata.org
99	IT-Lav	11.2813	45.9562	2003-2014 12y fluxnet.fluxdata.org
100	IT-MBo	11.0458	46.0147	2003-2013 11y Gilmanov et al. 2007
101	IT-Noe	8.1515	40.6061	2004-2014 11y fluxnet.fluxdata.org
102	IT-PT1	9.061	45.2009	2002-2004 3y Stoy et al. 2013
103	IT-Ren	11.4337	46.5869	1998-2013 16y Stoy et al. 2013
104	IT-Ro1	11.93	42.4081	2000-2008 9y Rey et al. 2002
105	IT-Ro2	11.9209	42.3903	2002-2012 11y Tedeschi et al. 2006
106	IT-SR2	10.291	43.732	2013-2014 2y fluxnet.fluxdata.org
107	IT-SRo	10.2844	43.7279	1999-2012 14y Reichstein et al. 2005
108	IT-Tor	7.5781	45.8444	2008-2014 7y Galvagno et al. 2013
109	JP-MBF	142.3186	44.3869	2003-2005 3y fluxnet.fluxdata.org
110	JP-SMF	137.0788	35.2617	2002-2006 5y fluxnet.fluxdata.org
111	NL-Hor	5.0713	52.2404	2004-2011 8y Sulkava et al. 2011
112	NL-Loo	5.7436	52.1666	1996-2013 18y Gash & Dolman 2003
113	NO-Adv	15.923	78.186	2011-2014 4y fluxnet.fluxdata.org
114	NO-Blv	11.8311	78.9216	2008-2009 2y fluxnet.fluxdata.org
115	RU-Che	161.3414	68.613	2002-2005 4y Merbold et al. 2009
116	RU-Cok	147.4943	70.8291	2003-2014 12y Stoy et al. 2013

ID	Longitude	Latitude	Years	Reference	
117	RU-Fyo	32.9221	56.4615	1998-2014 17y	Stoy et al. 2013
118	RU-Ha1	90.0022	54.7252	2002-2004 3y	Belelli Marchesini et al. 2007
119	SD-Dem	30.4783	13.2829	2005-2009 5y	Sjöström et al. 2009
120	SN-Dhr	-15.4322	15.4028	2010-2013 4y	Tagesson et al. 2015
121	US-AR1	-99.42	36.4267	2009-2012 4y	doi:10.17190/AMF/1246137
122	US-AR2	-99.5975	36.6358	2009-2012 4y	doi:10.17190/AMF/1246138
123	US-ARb	-98.0402	35.5497	2005-2006 2y	doi:10.17190/AMF/1246025
124	US-ARc	-98.04	35.5465	2005-2006 2y	doi:10.17190/AMF/1246026
125	US-ARM	-97.4888	36.6058	2003-2012 10y	doi:10.17190/AMF/1246027
126	US-Blo	-120.6328	38.8953	1997-2007 11y	doi:10.17190/AMF/1246032
127	US-Cop	-109.3900	38.0900	2001-2007 7y	doi:10.17190/AMF/1246129
128	US-GBT	-106.2397	41.3658	1999-2006 8y	Zeller & Hehn 1996
129	US-GLE	-106.2399	41.3665	2004-2014 11y	doi:10.17190/AMF/1246056
130	US-Ha1	-72.1715	42.5378	1991-2012 22y	doi:10.17190/AMF/1246059
131	US-KS2	-80.6715	28.6086	2003-2006 4y	doi:10.17190/AMF/1246070
132	US-Los	-89.9792	46.0827	2000-2014 15y	doi:10.17190/AMF/1246071
133	US-Me1	-121.5000	44.5794	2004-2005 2y	doi:10.17190/AMF/1246074
134	US-Me2	-121.5574	44.4523	2002-2014 13y	doi:10.17190/AMF/1246076
135	US-Me6	-121.6078	44.3233	2010-2014 5y	doi:10.17190/AMF/1246128
136	US-MMS	-86.4131	39.3232	1999-2014 16y	doi:10.17190/AMF/1246080
137	US-Myb	-121.7651	38.0498	2010-2014 5y	doi:10.17190/AMF/1246139
138	US-Ne1	-96.4766	41.1651	2001-2013 13y	doi:10.17190/AMF/1246084
139	US-Ne2	-96.4701	41.1649	2001-2013 13y	doi:10.17190/AMF/1246085
140	US-Ne3	-96.4397	41.1797	2001-2013 13y	doi:10.17190/AMF/1246086
141	US-NR1	-105.5464	40.0329	1998-2014 17y	doi:10.17190/AMF/1246088
142	US-ORv	-83.0183	40.0201	2011-2011 1y	doi:10.17190/AMF/1246135
143	US-PFa	-90.2723	45.9459	1995-2014 20y	doi:10.17190/AMF/1246090
144	US-Prr	-147.4876	65.1237	2010-2013 4y	doi:10.17190/AMF/1246153
145	US-SRG	-110.8277	31.7894	2008-2014 7y	doi:10.17190/AMF/1246154
146	US-SRM	-110.8661	31.8214	2004-2014 11y	doi:10.17190/AMF/1246104
147	US-Syv	-89.3477	46.2420	2001-2014 14y	doi:10.17190/AMF/1246106
148	US-Ton	-120.966	38.4316	2001-2014 14y	doi:10.17190/AMF/1245941
149	US-Tw1	-121.6469	38.1074	2012-2014 3y	doi:10.17190/AMF/1246147
150	US-Tw2	-121.6433	38.1047	2012-2013 2y	doi:10.17190/AMF/1246148
151	US-Tw3	-121.6467	38.1159	2013-2014 2y	doi:10.17190/AMF/1246149
152	US-Tw4	-121.6414	38.1030	2013-2014 2y	doi:10.17190/AMF/1246151
153	US-Twt	-121.6530	38.1087	2009-2014 6y	doi:10.17190/AMF/1246140
154	US-UMB	-84.7138	45.5598	2000-2014 15y	doi:10.17190/AMF/1246107
155	US-UMd	-84.6975	45.5625	2007-2014 8y	doi:10.17190/AMF/1246134

ID	Longitude	Latitude	Years	Reference
156 US-Var	-120.9507	38.4133	2000-2014 15y	doi:10.17190/AMF/1245984
157 US-WCr	-90.0799	45.8059	1999-2014 16y	doi:10.17190/AMF/1246111
158 US-Whs	-110.0522	31.7438	2007-2014 8y	doi:10.17190/AMF/1246113
159 US-Wi0	-91.0814	46.6188	2002-2002 1y	doi:10.17190/AMF/1246116
160 US-Wi3	-91.0987	46.6347	2002-2004 3y	doi:10.17190/AMF/1246118
161 US-Wi4	-91.1663	46.7393	2002-2005 4y	doi:10.17190/AMF/1246019
162 US-Wi6	-91.2982	46.6249	2002-2003 2y	doi:10.17190/AMF/1246121
163 US-Wi9	-91.0814	46.6188	2004-2005 2y	doi:10.17190/AMF/1246024
164 US-Wkg	-109.9419	31.7365	2004-2014 11y	doi:10.17190/AMF/1246112
165 ZA-Kru	31.4969	-25.0197	2000-2010 11y	King et al. 2003
166 ZM-Mon	23.2528	-15.4378	2000-2009 10y	King et al. 2003

Table S2. Gridded observed precipitation products used for comparison of annual totals to FLUXNET2015 observations in Figure 2. Time span is “entire” if the data cover the range Jan1991-Dec2014, which is the maximum span of FLUXNET2015.

Product	Time Span	Resolution	Primary Reference
GPCP 2.2	Entire	2.5°	Adler et al. (2003)
1DD 1.2	Oct 1996 onward	1°	Huffman et al. (2001)
MSWEP 1.0	Entire	0.25°	Beck et al. (2017)
CPC-Uni	Entire	0.5°	Xie et al. (2007)
U.Del 4.01	Entire	1°	Matsuura and Willmott (2014)
TRMM 3B43 v7	Jan 1998 onward	0.25°	Huffman et al. (2007)
WFDEI-CRU	Entire	0.5°	Weedon et al. (2011)
WFDEI-GPCC	Entire	0.5°	Weedon et al. (2011)

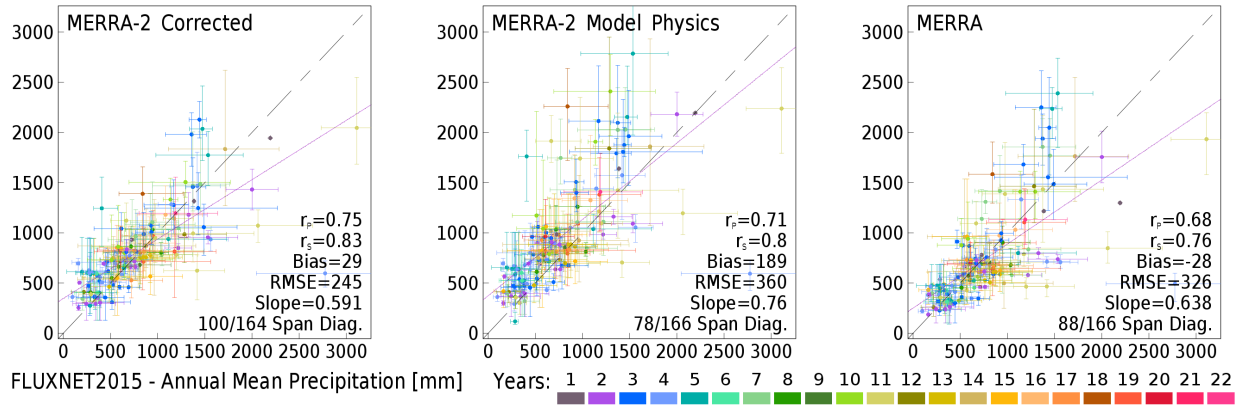


Figure S1: As in the bottom row of Fig 2, where “MERRA-2 Corrected” is the same as the panel labeled “MERRA-2” in Fig 2, but “MERRA-2 Model Physics” is the predicted precipitation rate from the GCM without correction. MERRA is also shown for comparison.

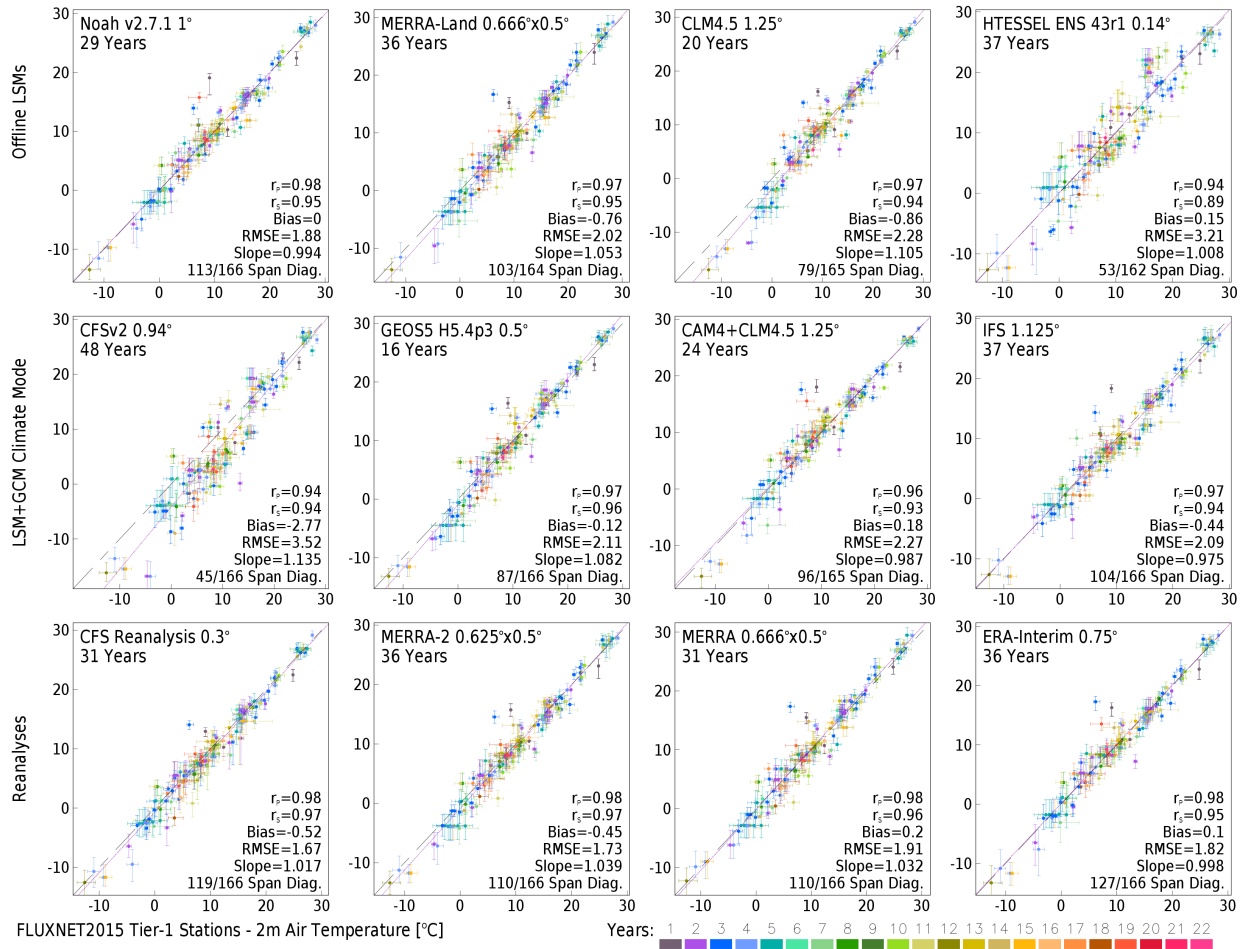


Figure S2: Scatter of annual mean 2m air temperature at FLUXNET2015 sites (abscissa) to multi-decade climatologies (ordinate; number of years given in upper left of each panel) from offline LSM simulations (top row), coupled LSM+GCM simulations (middle row) or reanalyses constrained by data assimilation (bottom row) using the value from the grid box containing the FLUXNET2015 site location (unless data are missing or indicated to be an all-ocean grid box). Dash-dotted diagonal grey line indicates X=Y. Colors indicate years of available data from each FLUXNET2015 site, whiskers span range of annual totals from FLUXNET2015 (horizontal) or models (vertical) for all available years. Purple line is the best-fit linear regression of Y on X. Statistics are explained in the main text.

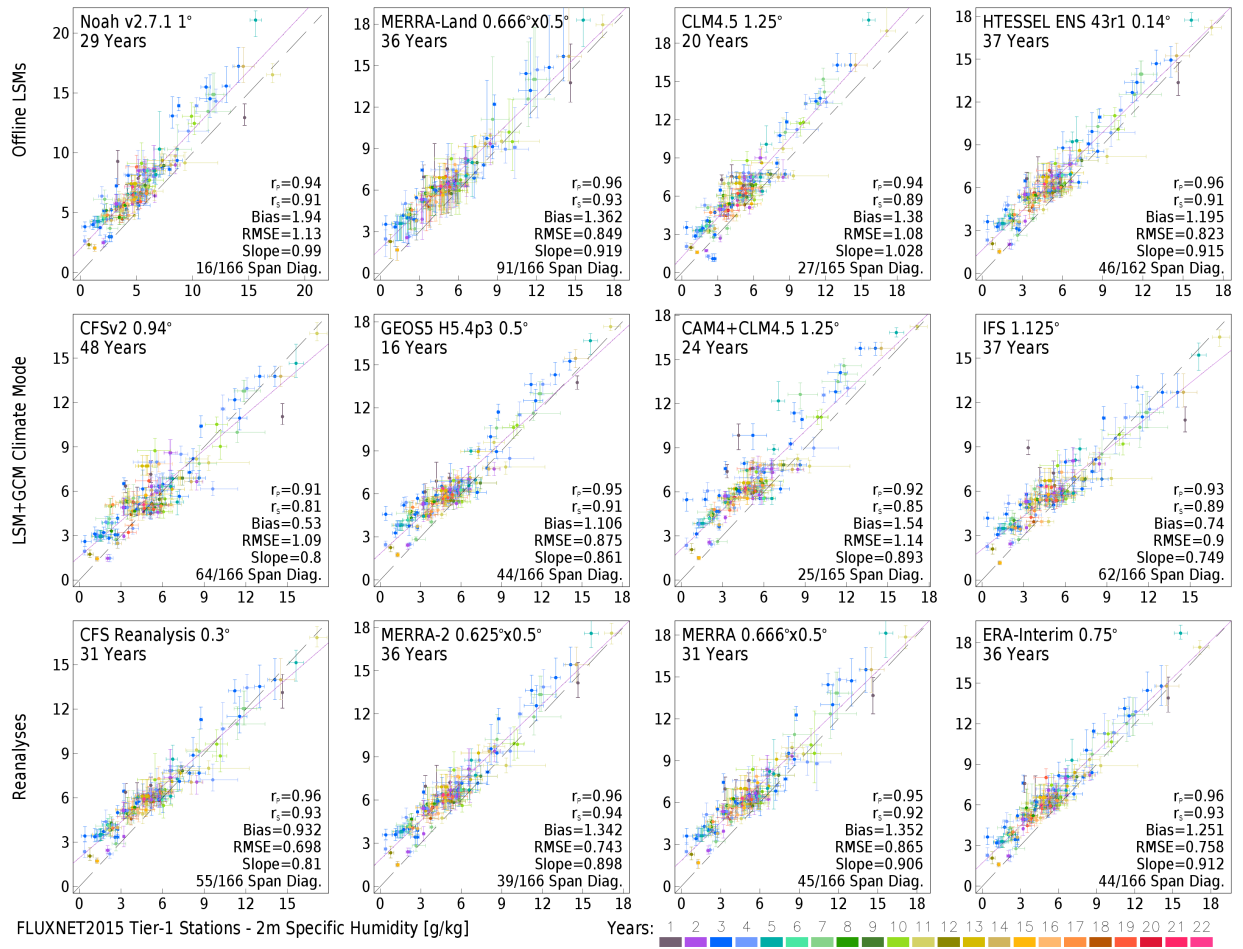


Figure S3: As in Fig S2 for 2m specific humidity.

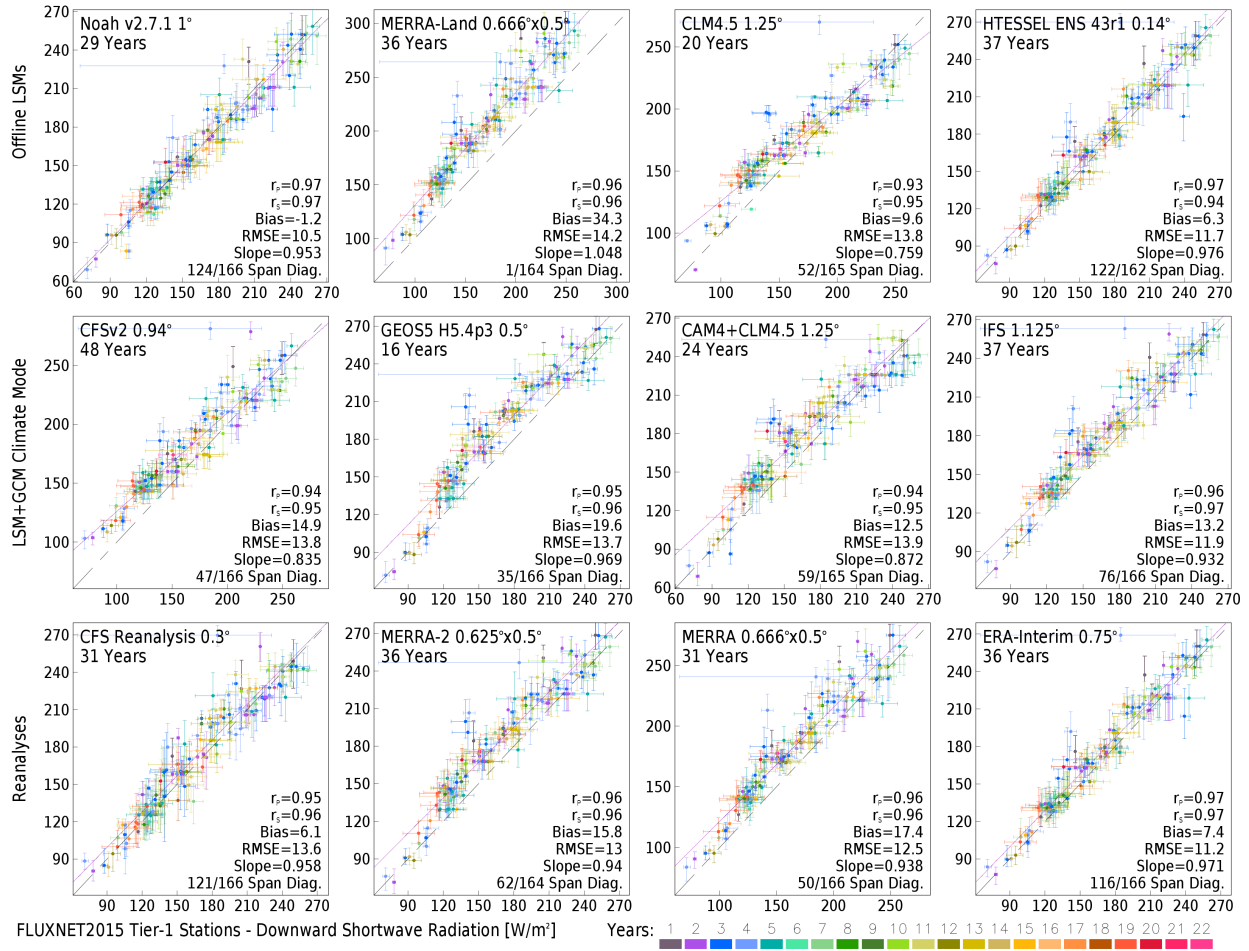


Figure S4: As in Fig S2 for downward shortwave radiation at the surface.

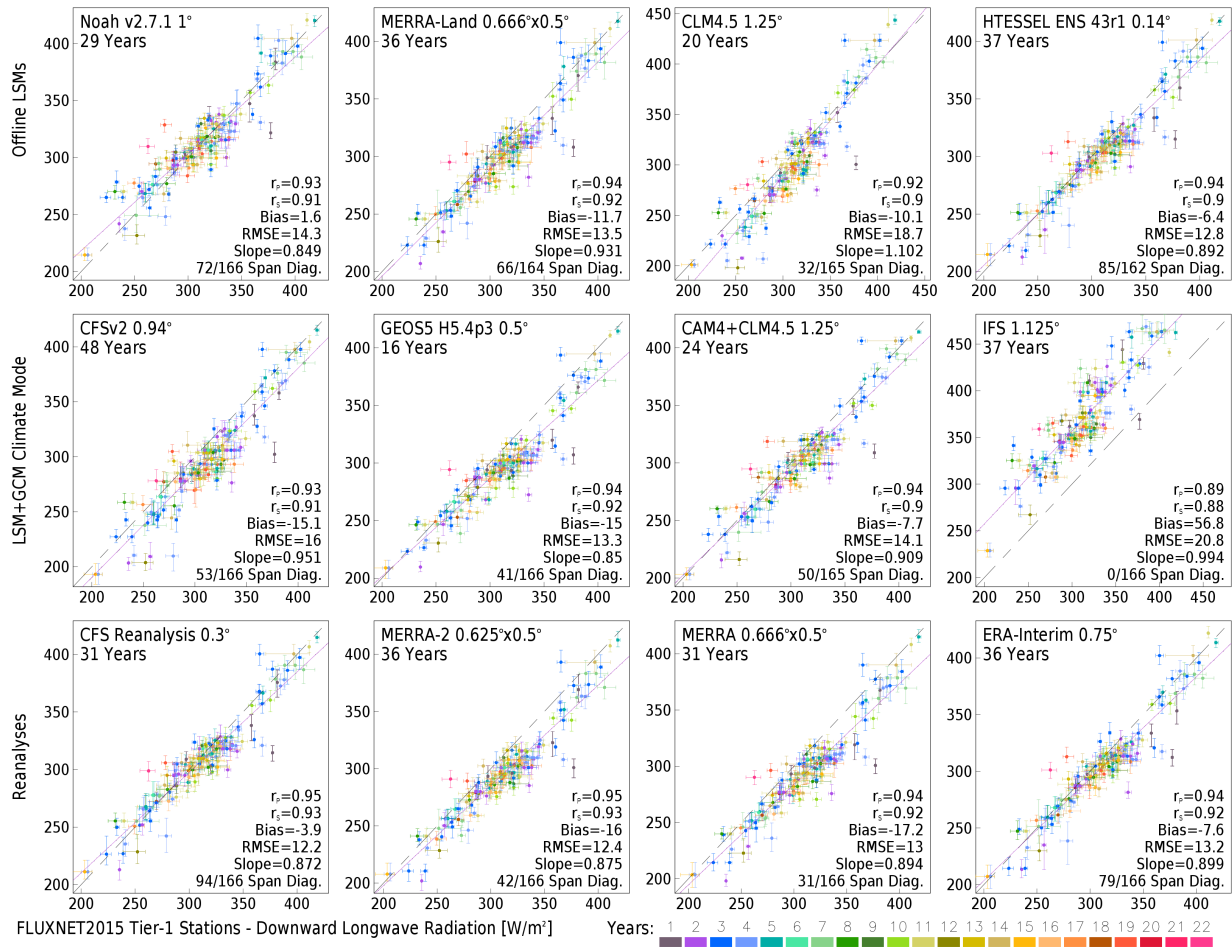


Figure S5: As in Fig S2 for downward longwave radiation at the surface.

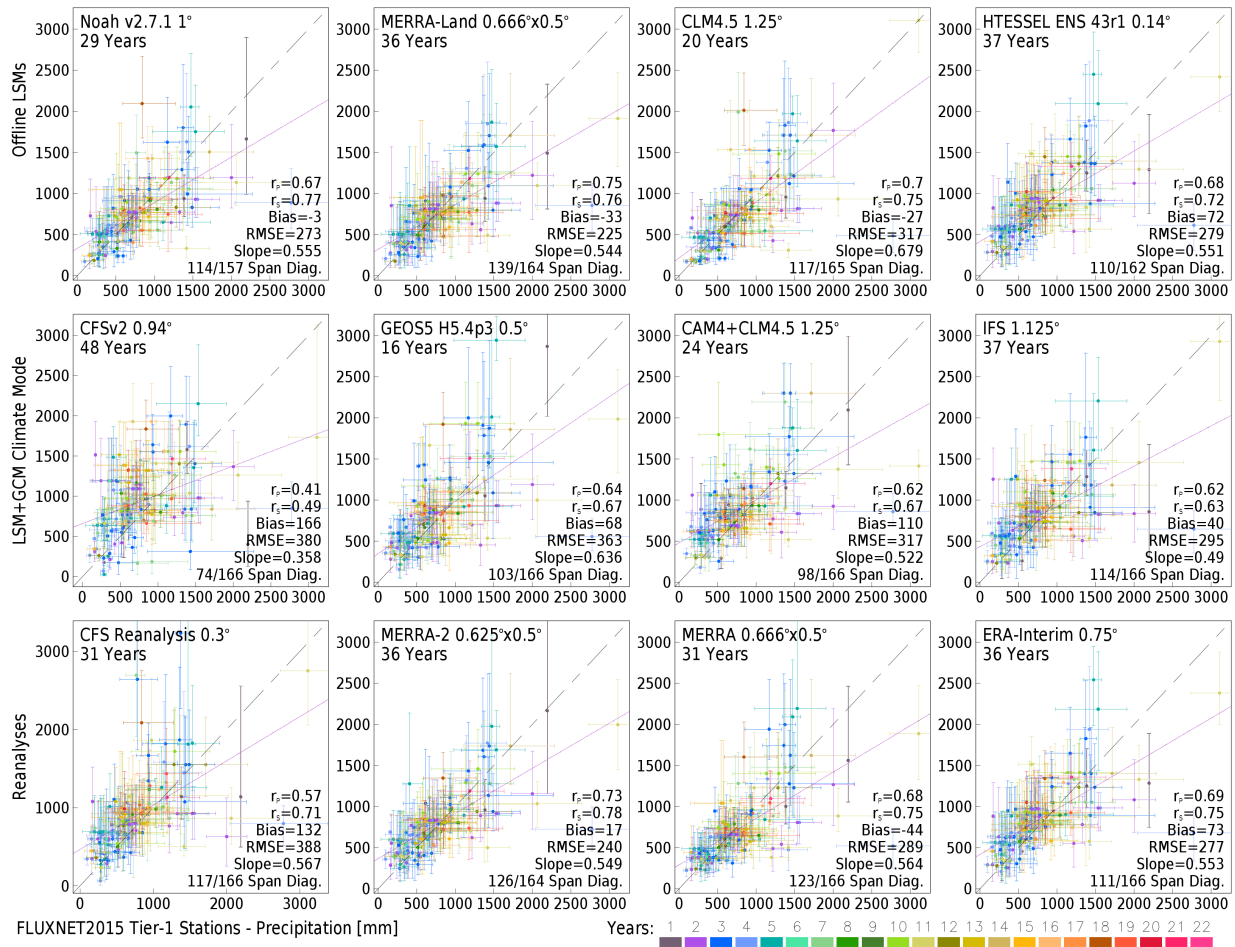


Figure S6: As in Fig S2 for precipitation.

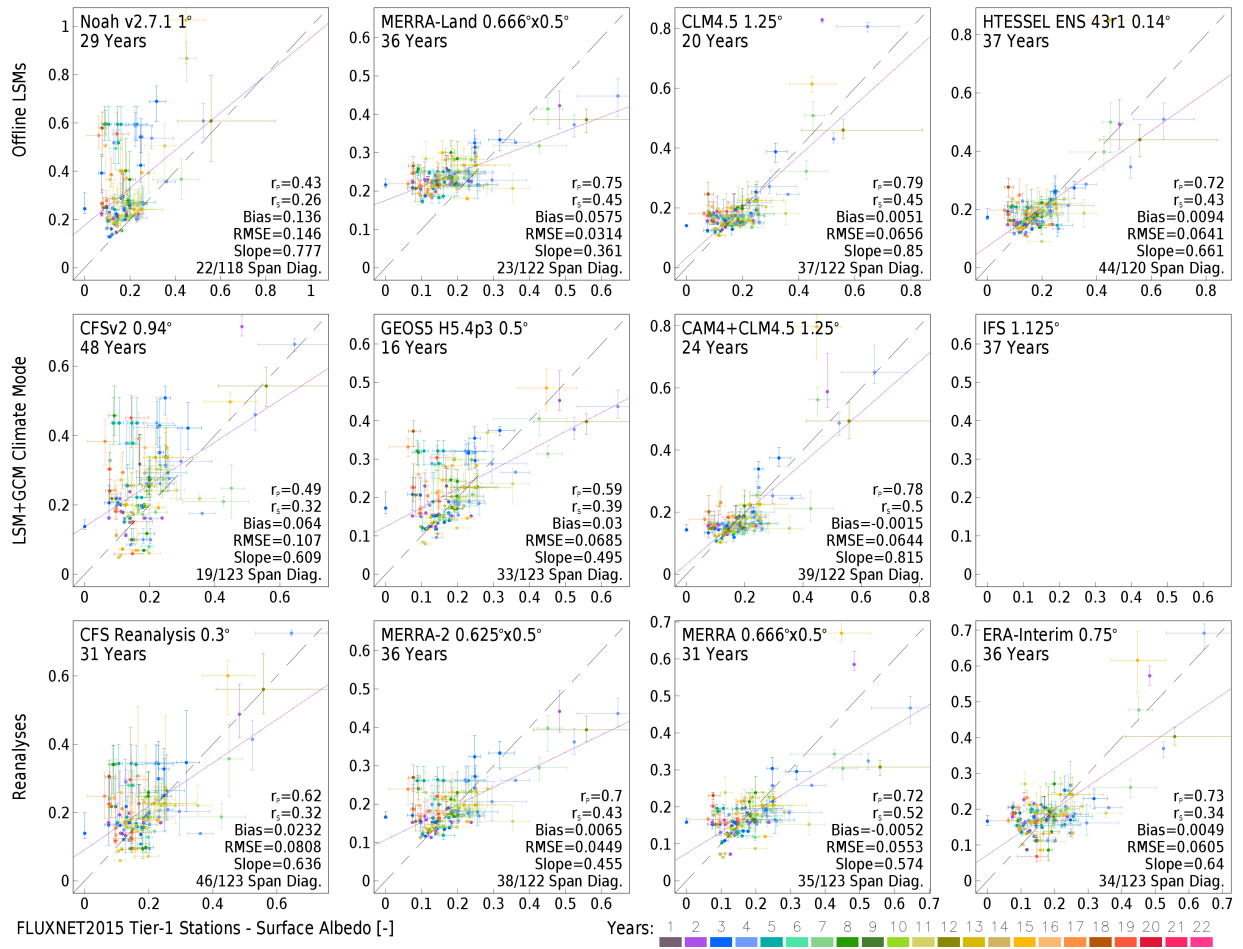


Figure S7: As in Fig S2 for surface albedo. Insufficient output to calculate albedo was available from the IFS simulation.

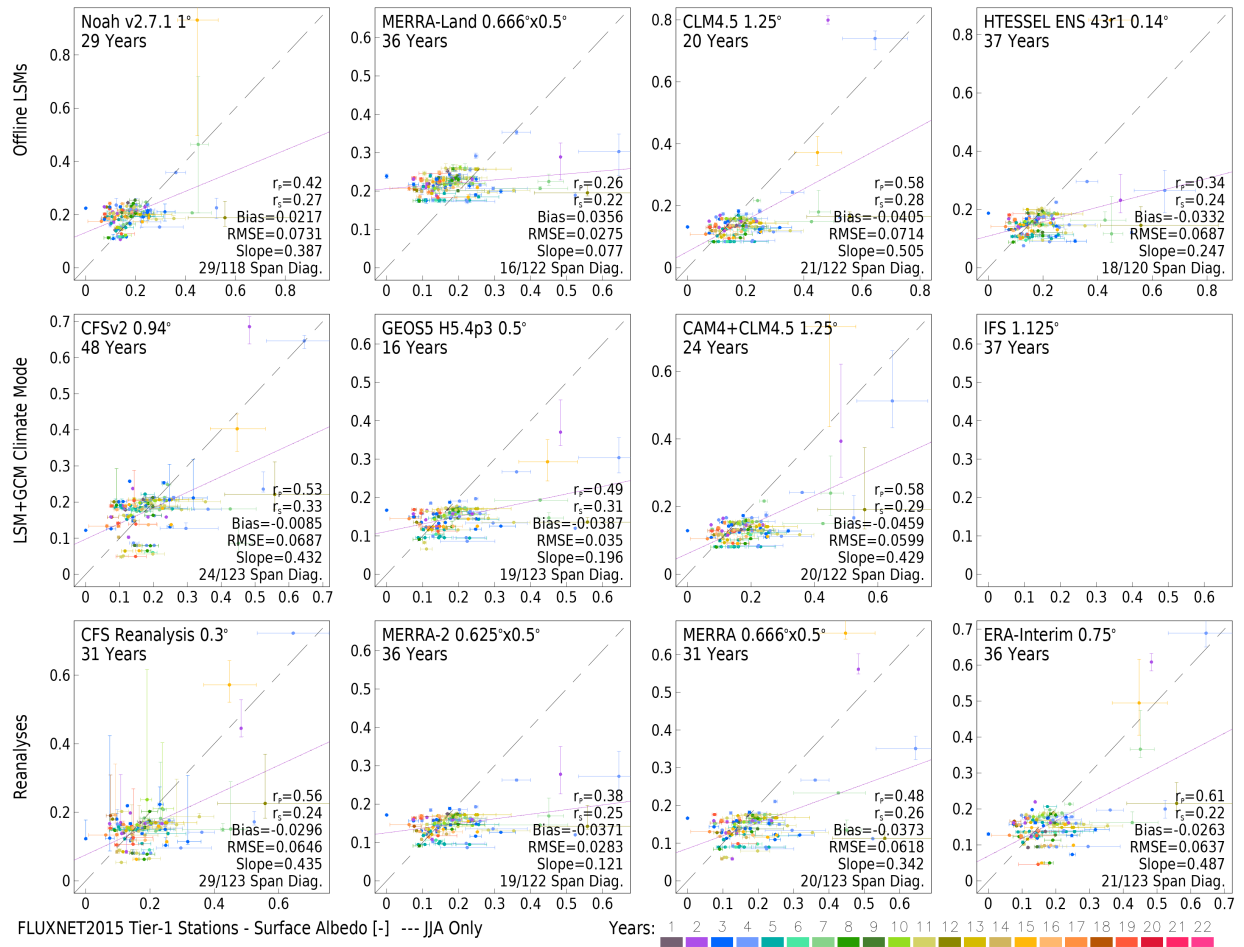


Figure S8: As in Fig S7 for surface albedo during JJA only. Insufficient output to calculate albedo was available from the IFS simulation.

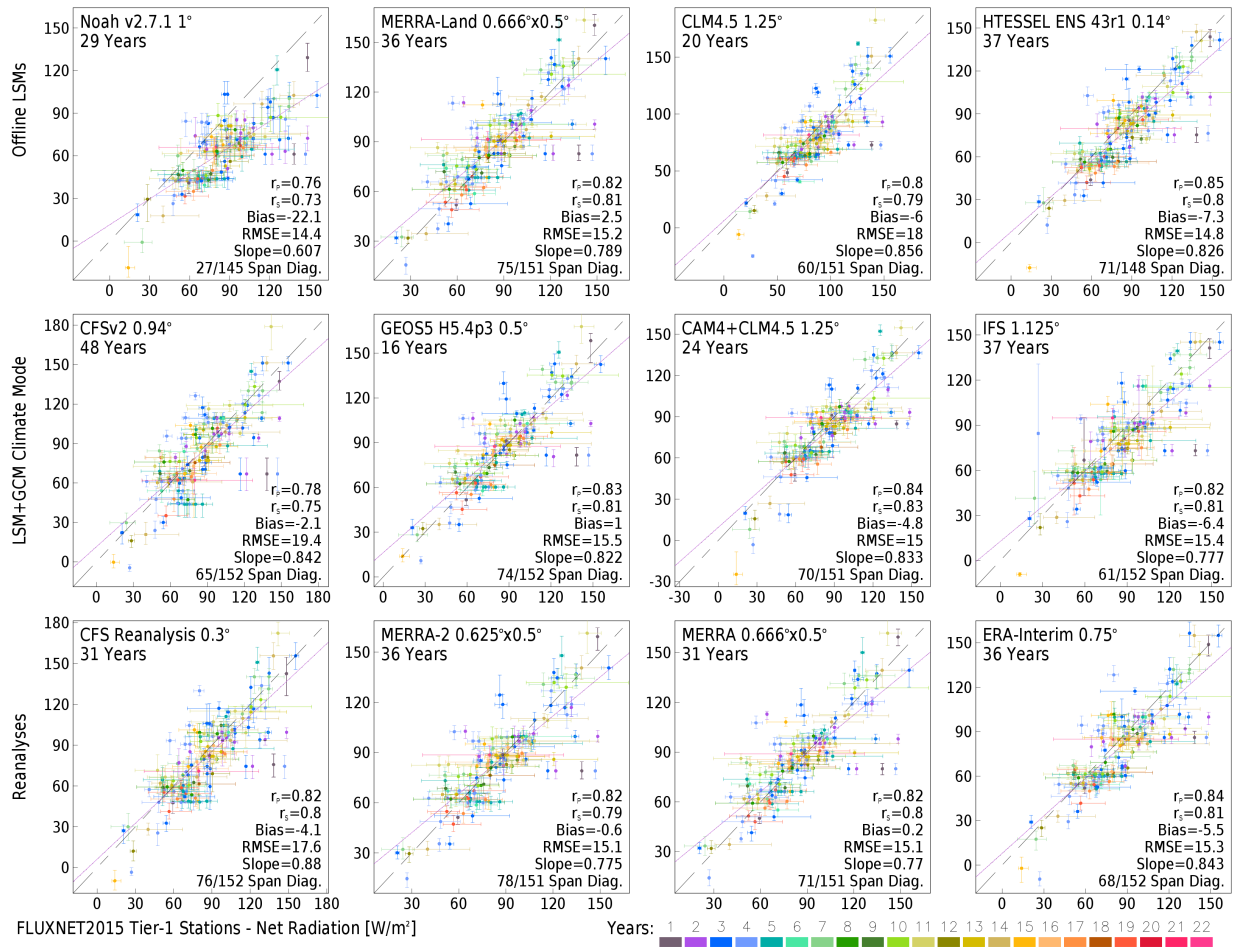


Figure S9: As in Fig S2 for net radiation at the surface (positive downward).

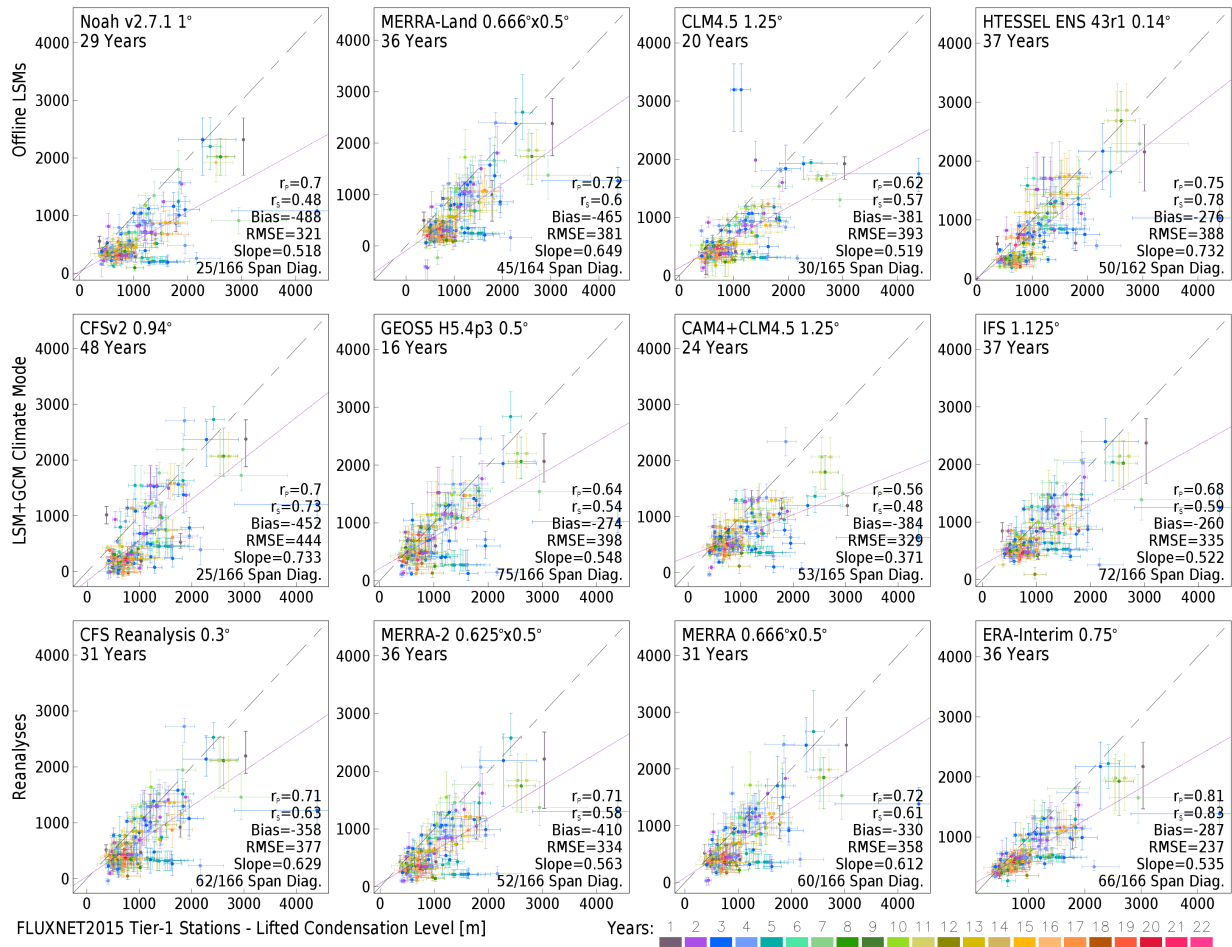


Figure S10: As in Fig S2 for lifting condensation level.

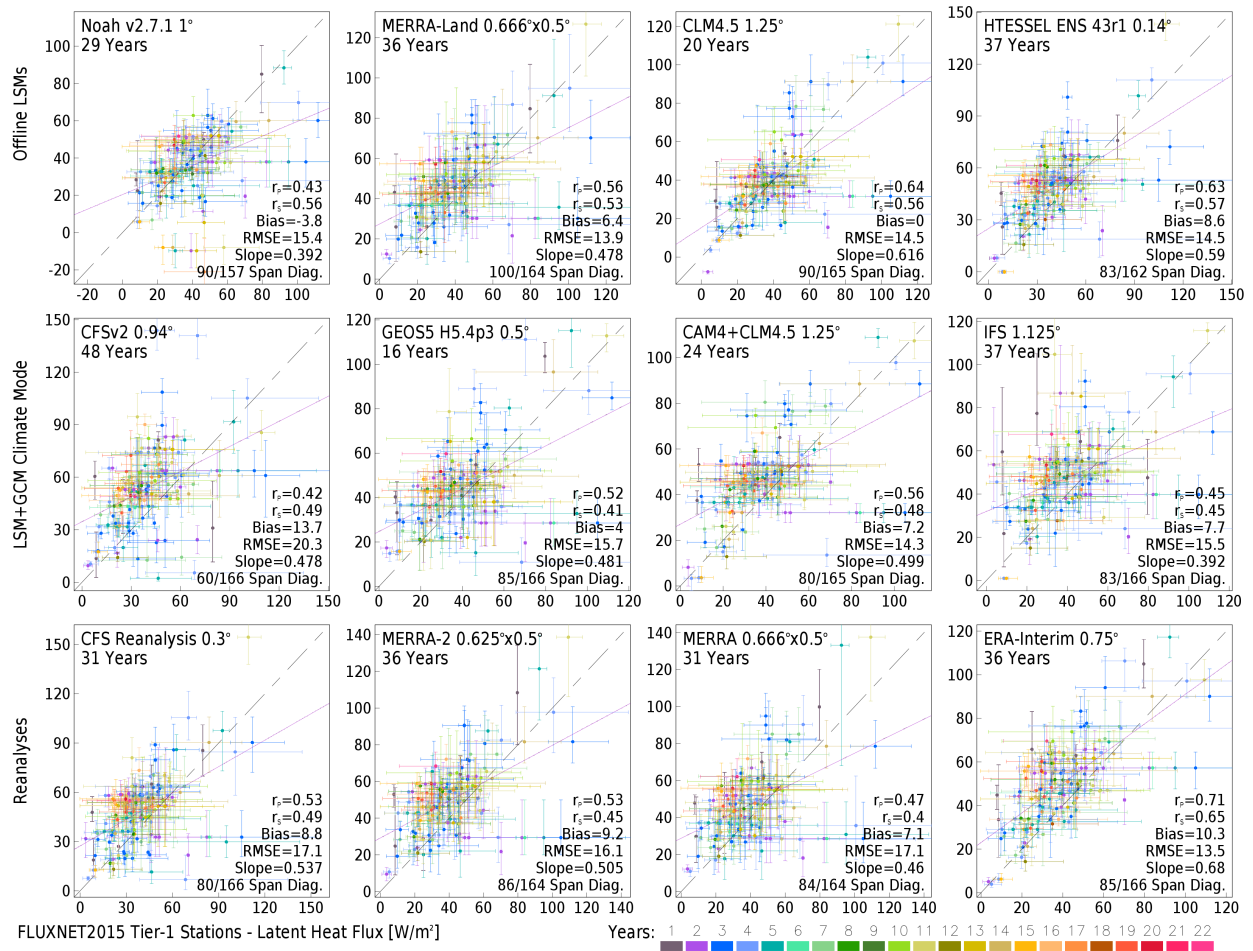


Figure S11: As in Fig S2 for latent heat flux (positive upward).

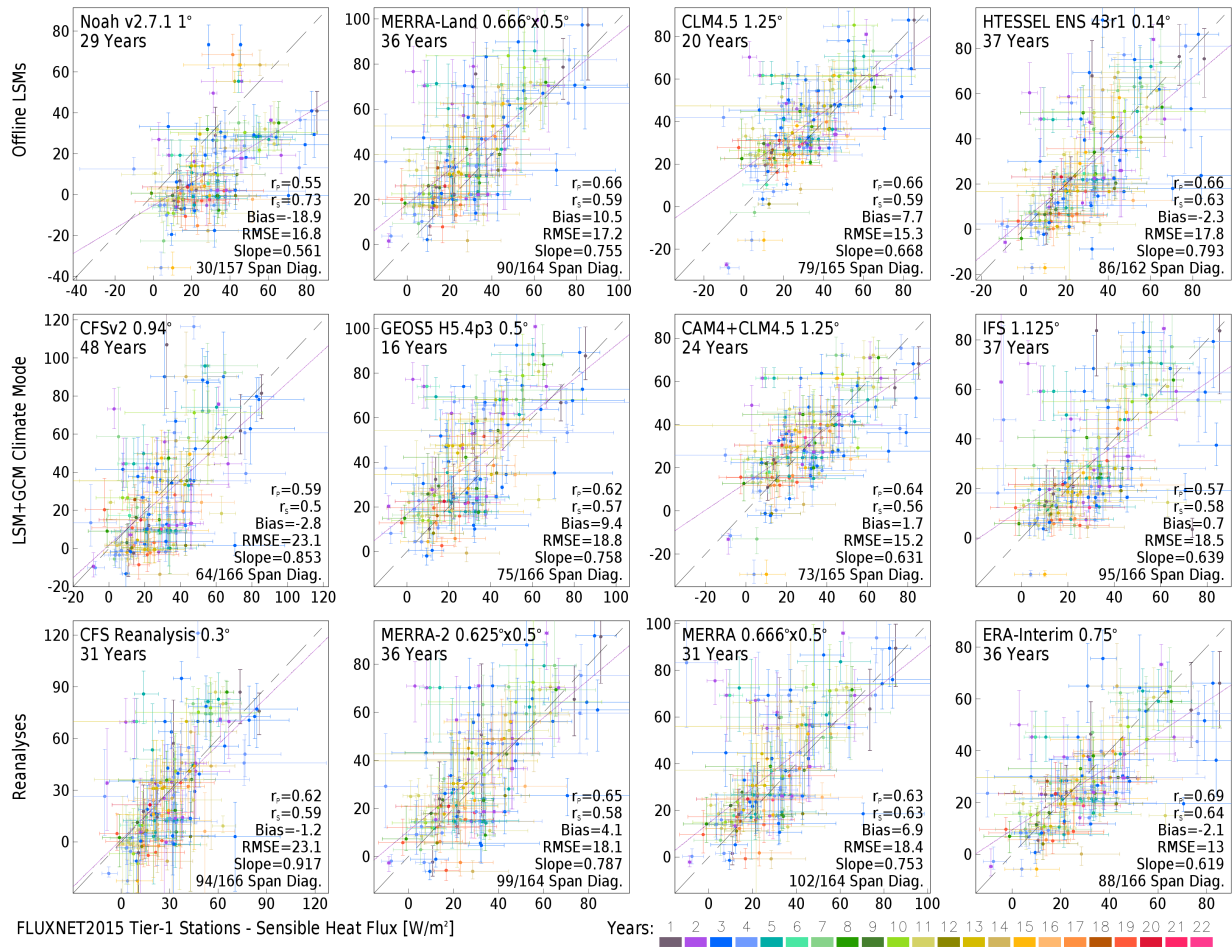


Figure S12: As in Fig S2 for sensible heat flux (positive upward).

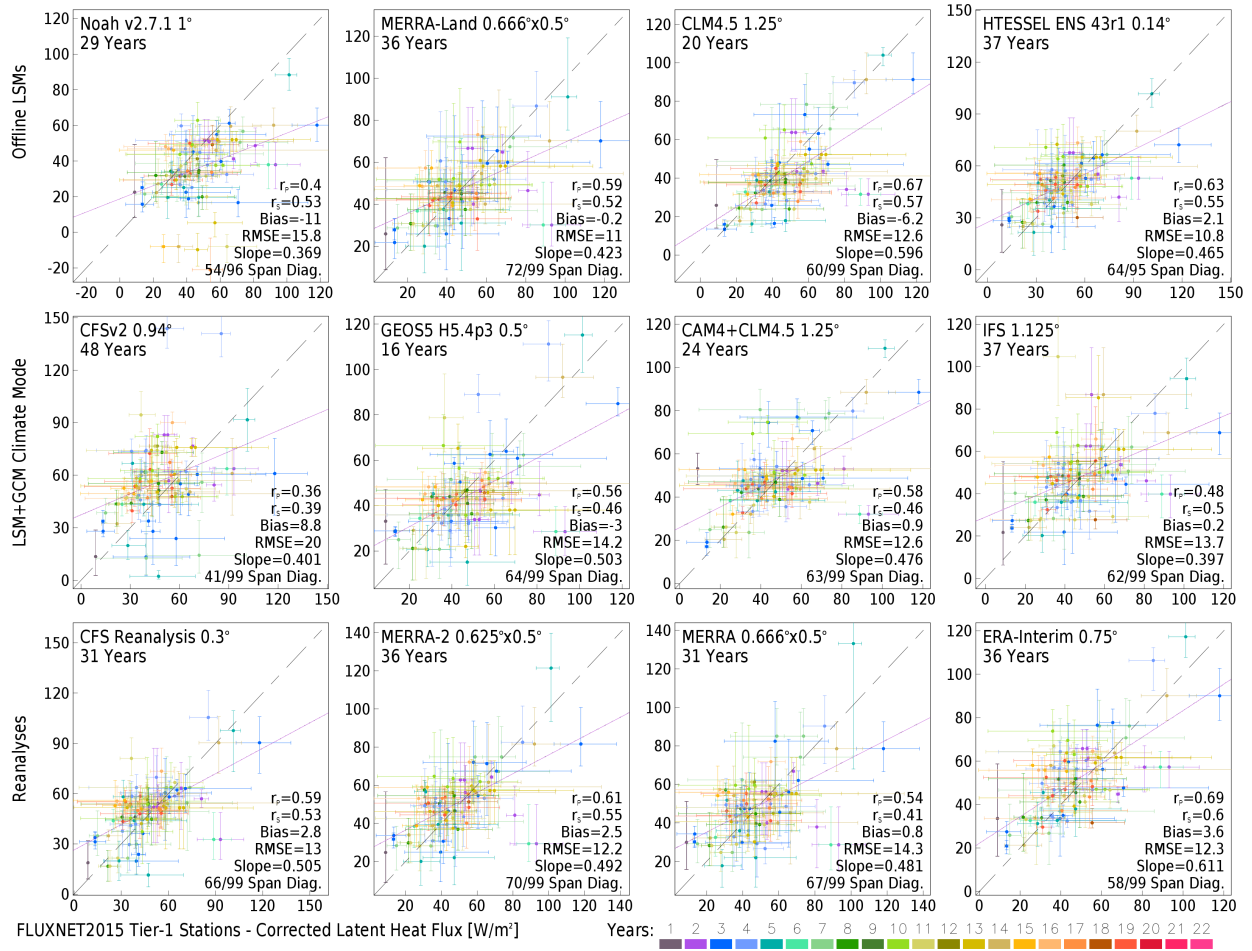


Figure S13: As in Fig S2 for latent heat flux corrected for surface energy balance closure (positive upward).

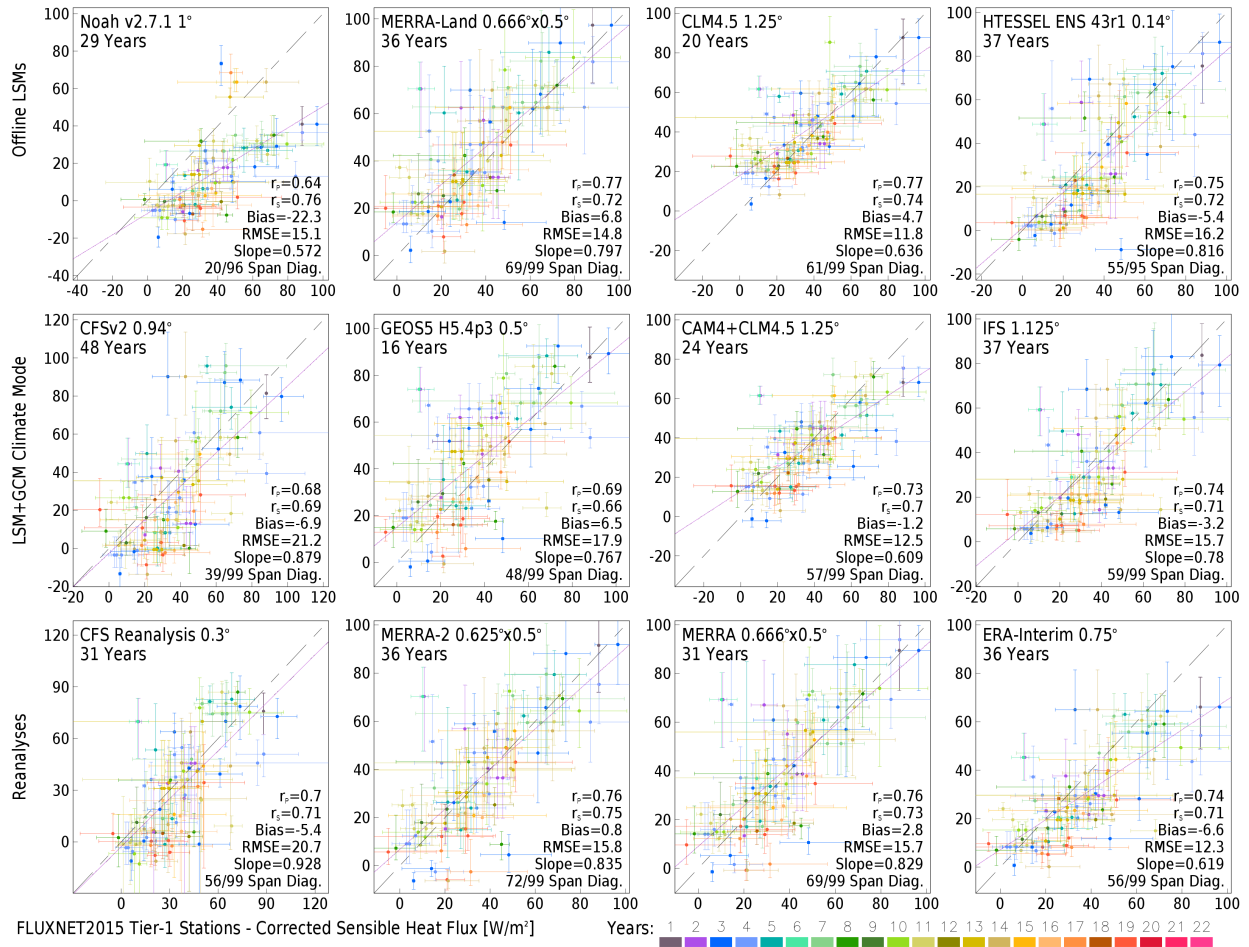


Figure S14: As in Fig S2 for sensible heat flux corrected for surface energy balance closure (positive upward).

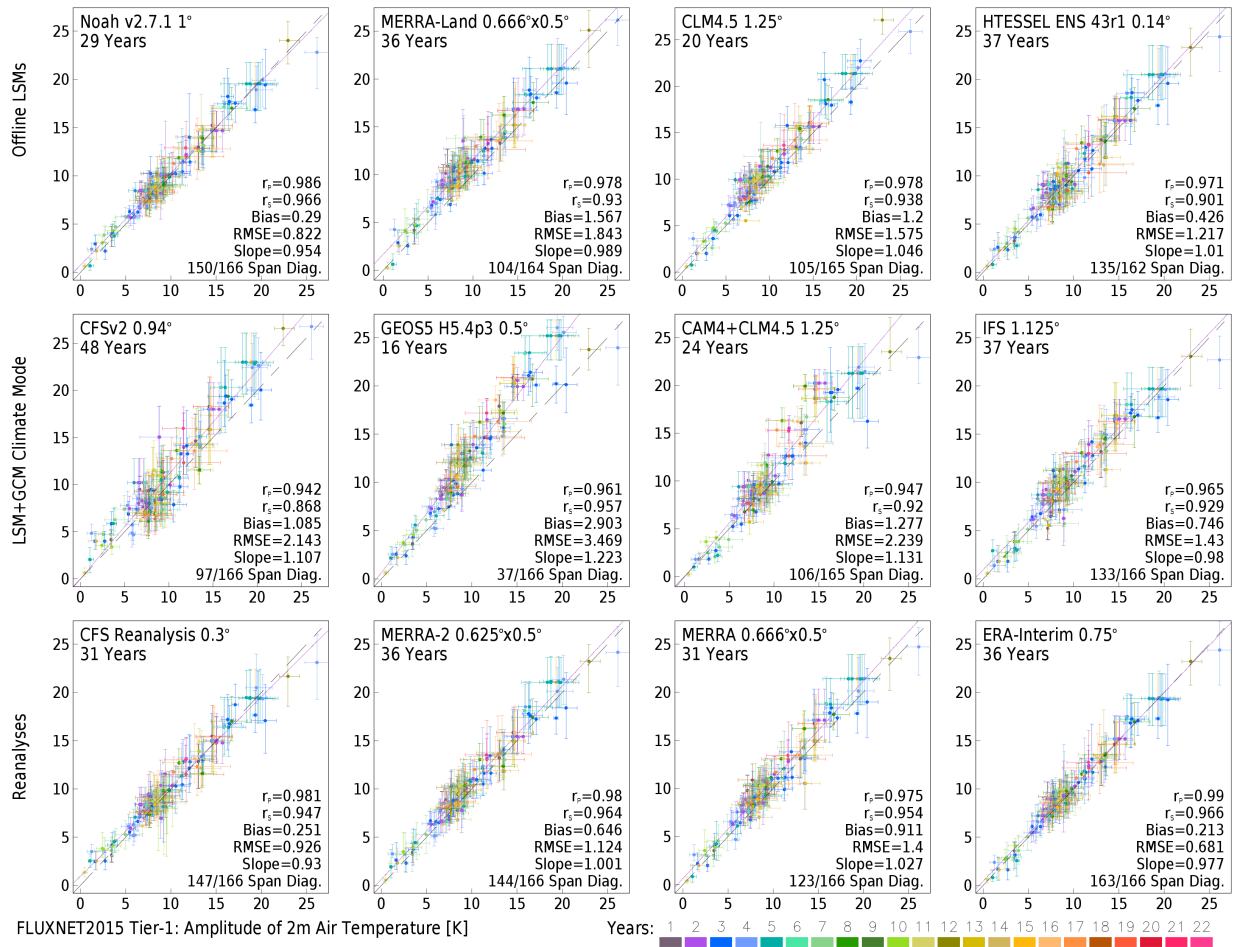


Figure S15: As in Fig S2 for the magnitude of the annual cycle (first harmonic calculated from monthly means) of 2m air temperature.

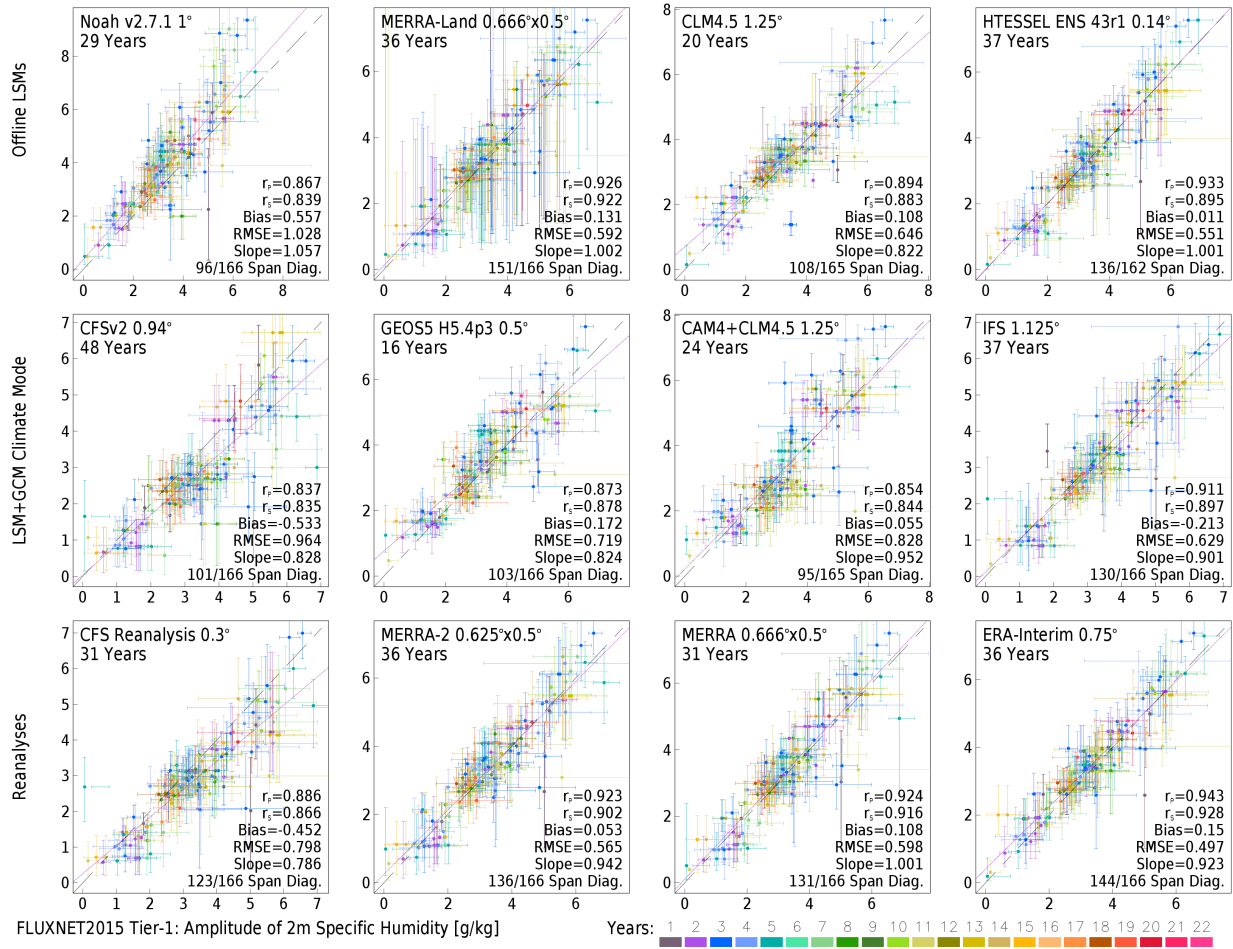


Figure S16: As in Fig S15 for 2m specific humidity.

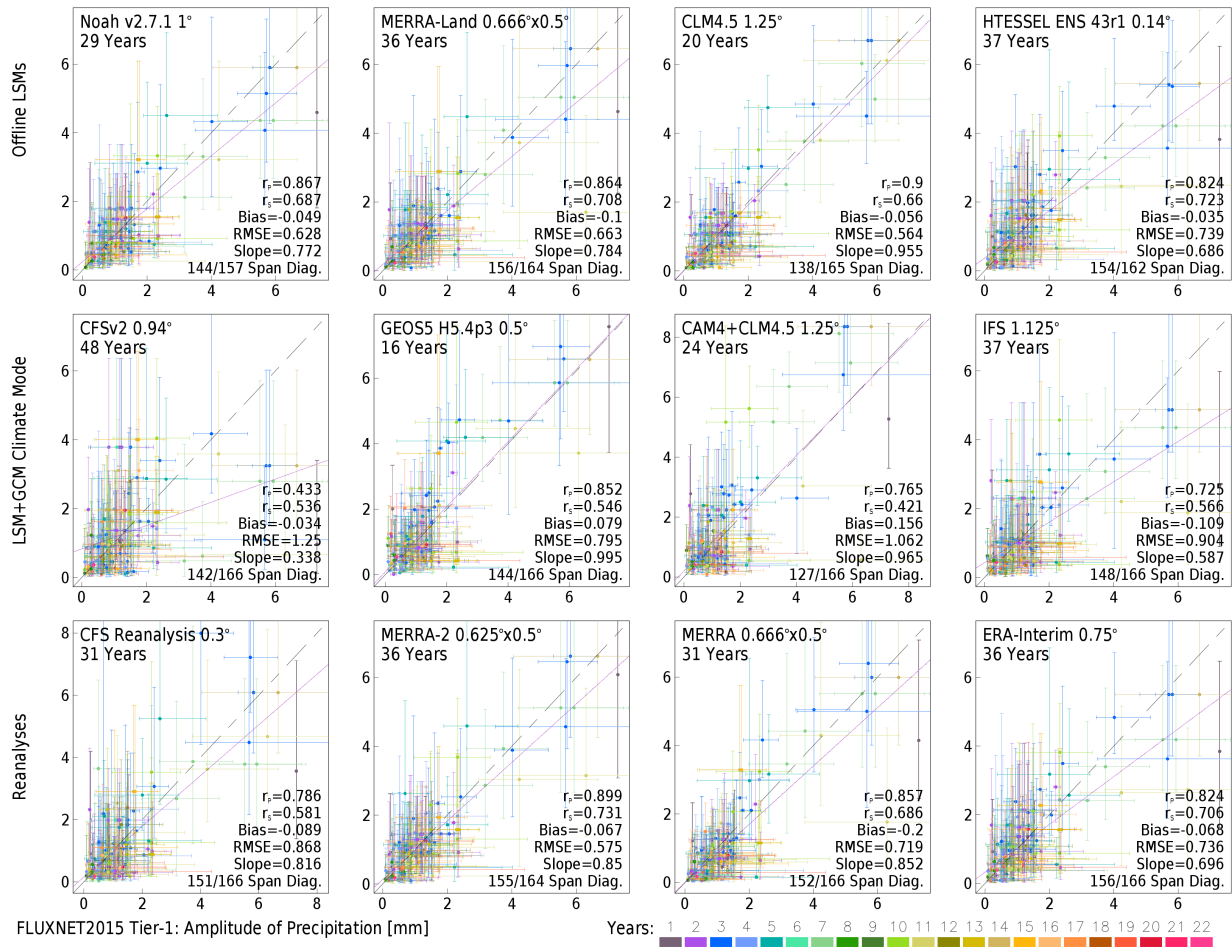


Figure S17: As in Fig S15 for precipitation.

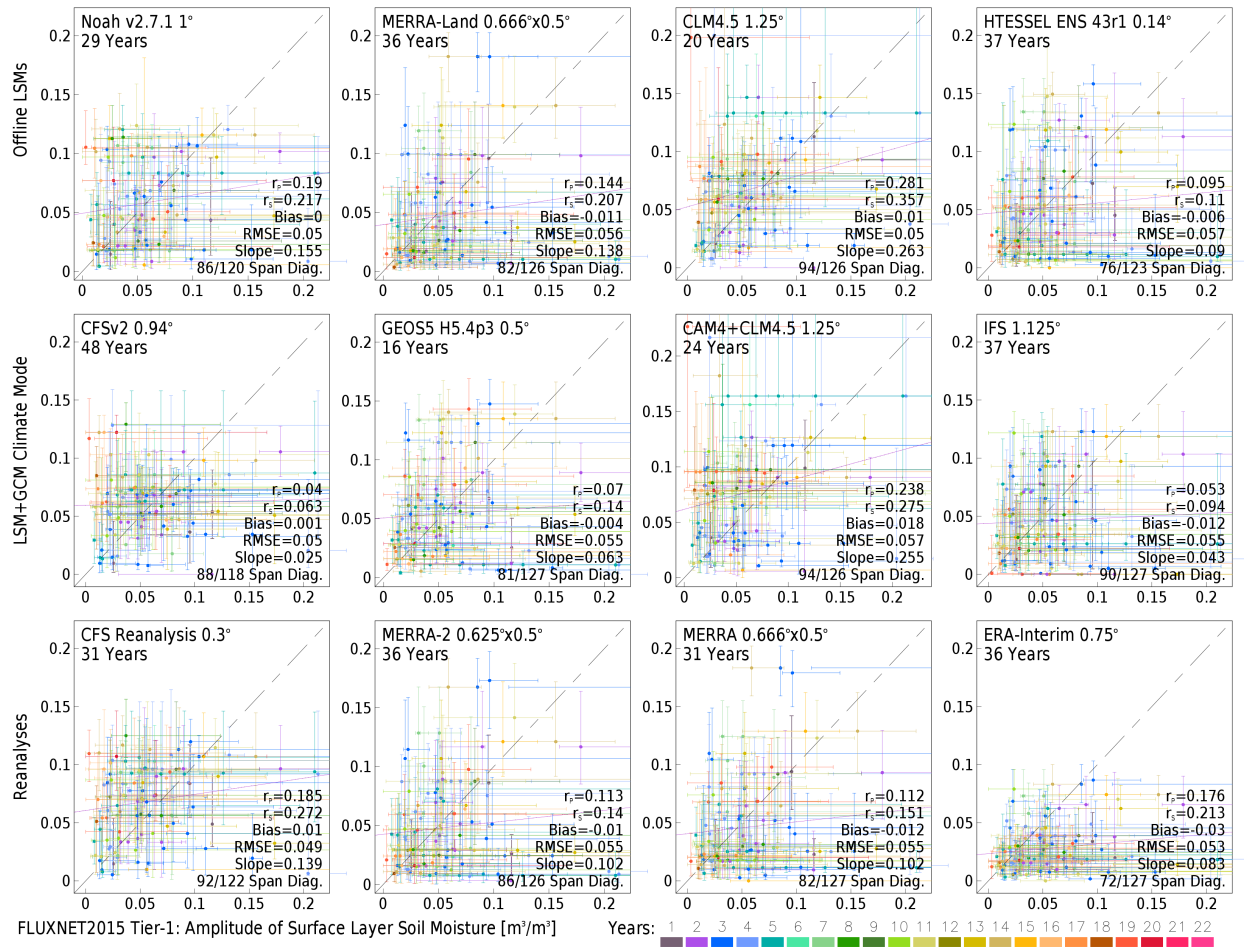


Figure S18: As in Fig S15 for near-surface volumetric soil moisture.

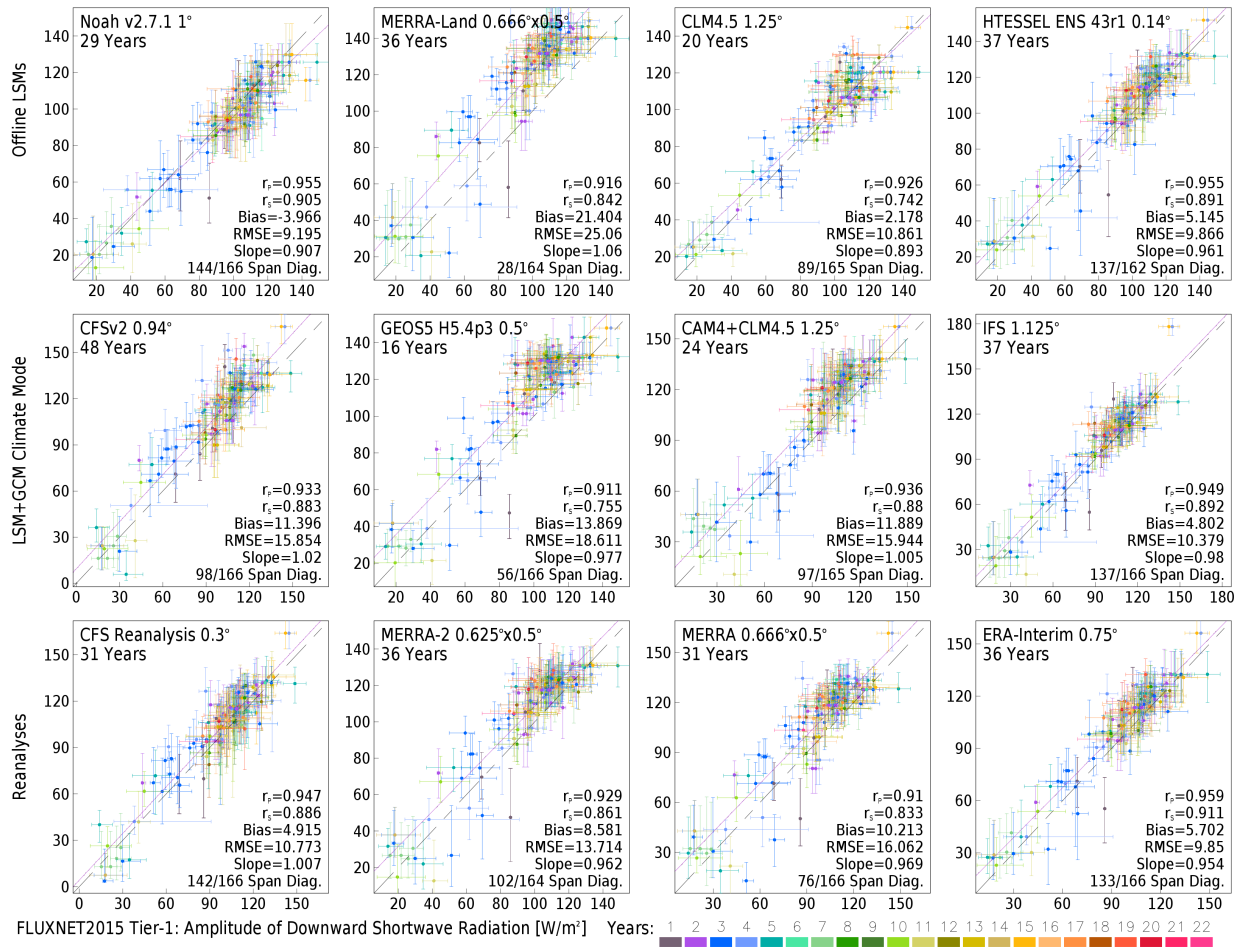


Figure S19: As in Fig S15 for downward shortwave radiation at the surface.

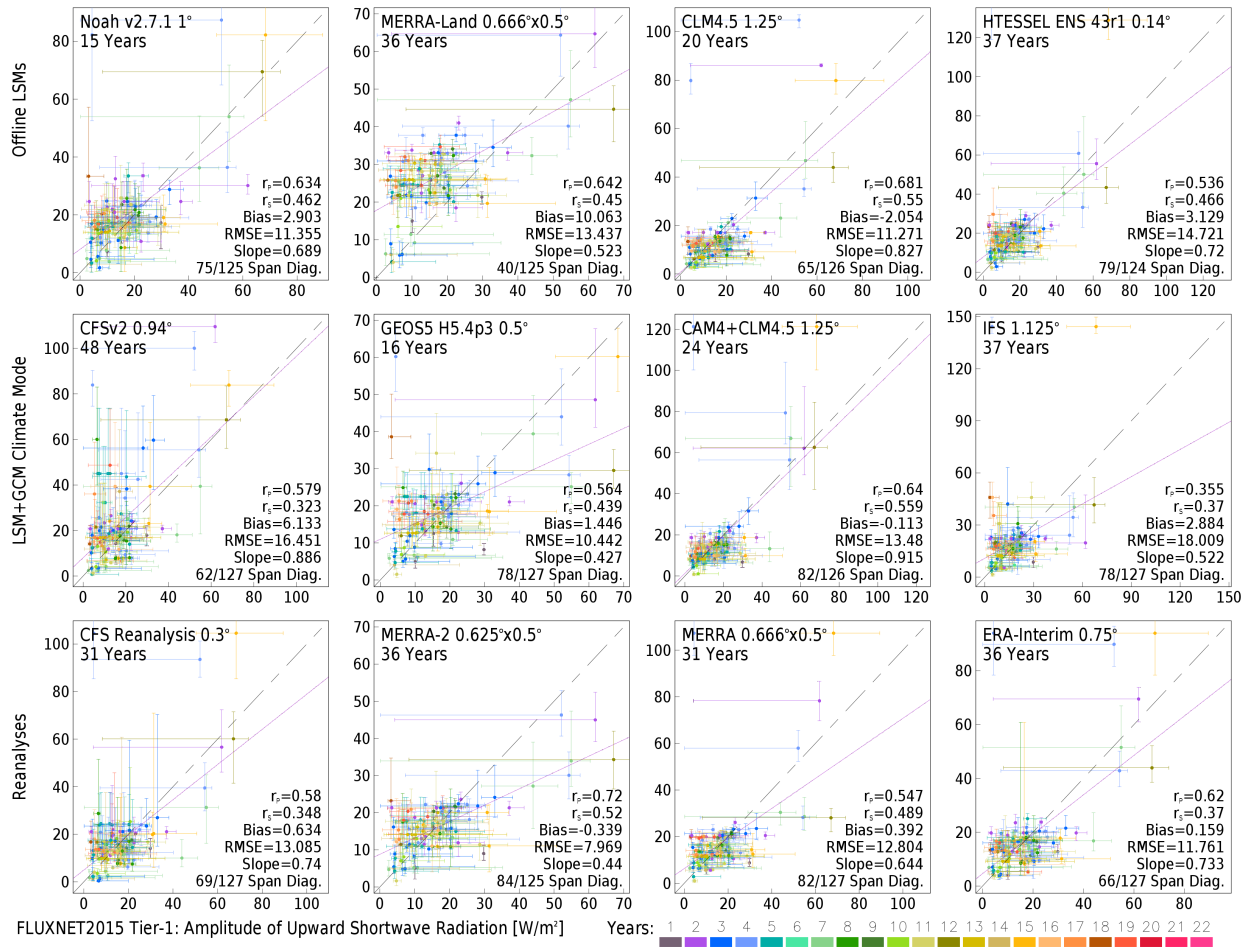


Figure S20: As in Fig S15 for upward shortwave radiation at the surface.

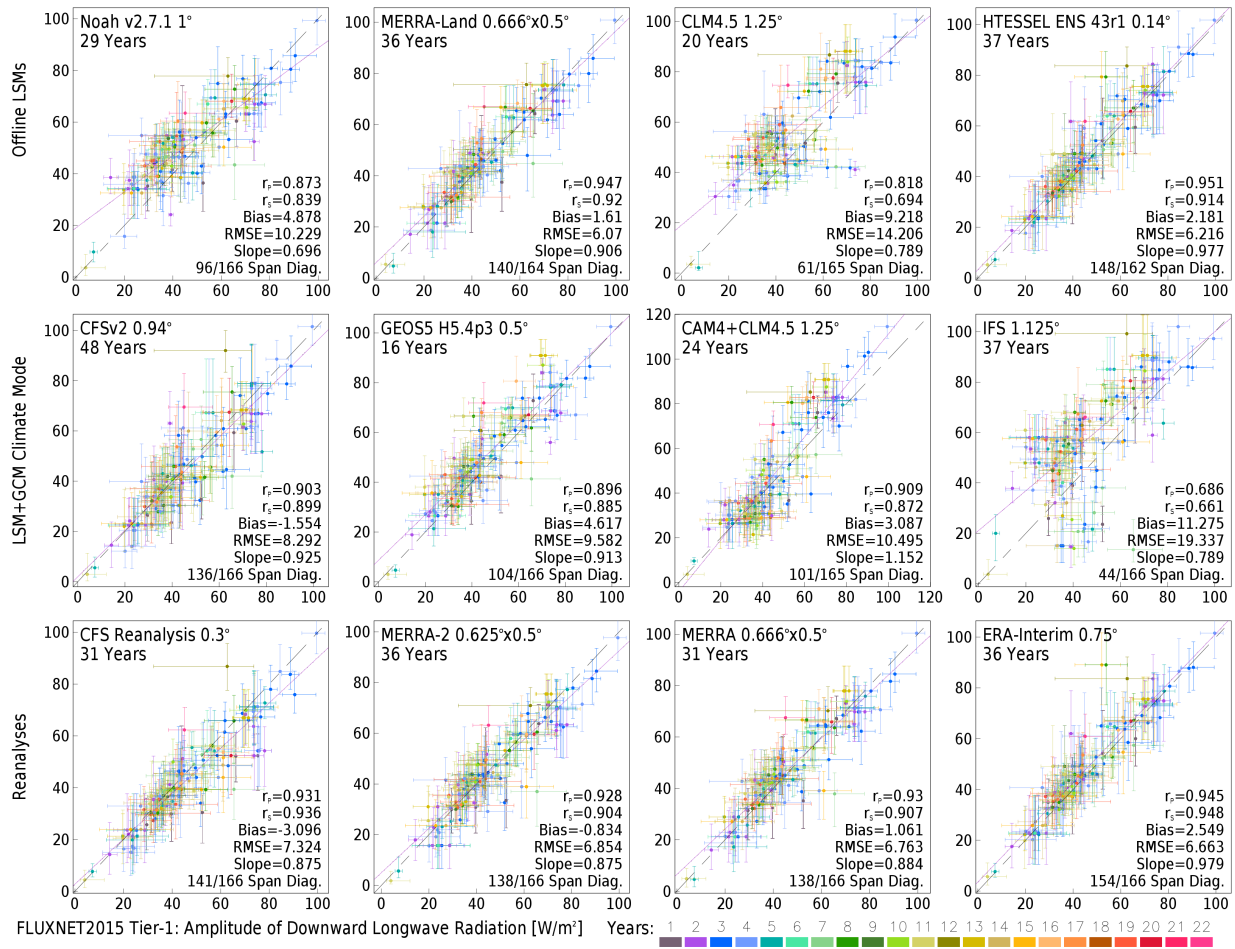


Figure S21: As in Fig S15 for downward longwave radiation at the surface.

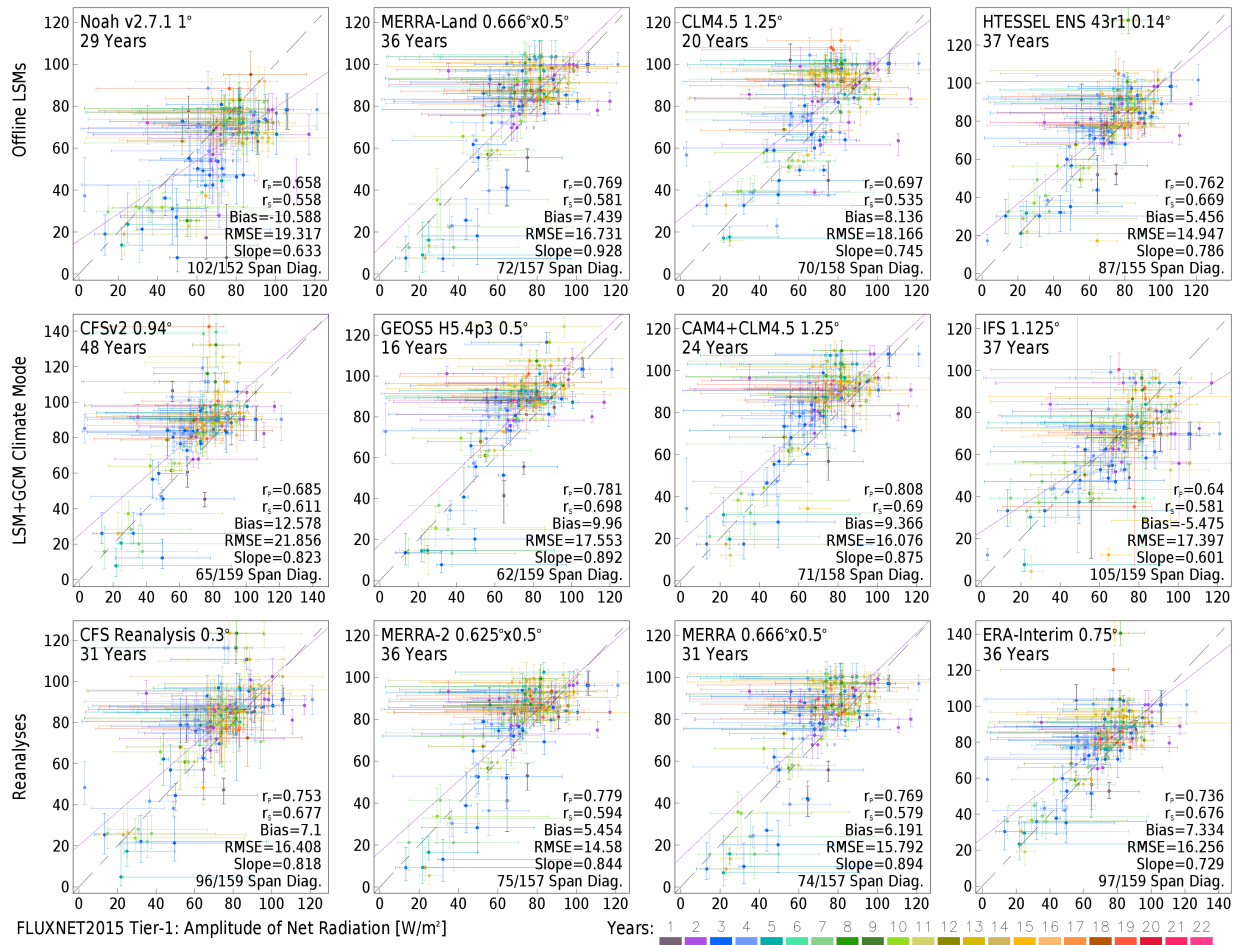


Figure S22: As in Fig S15 for net radiation at the surface (positive downward).

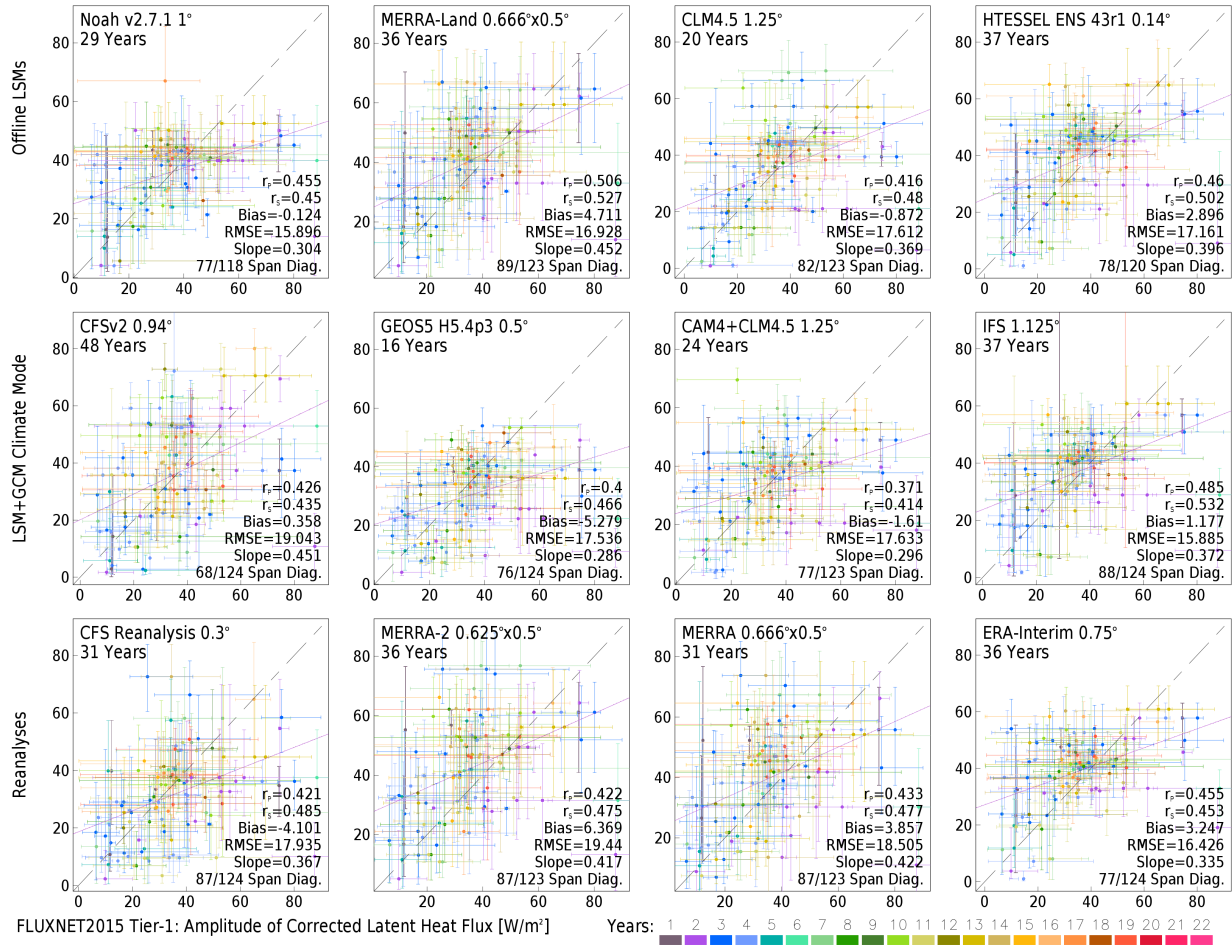


Figure S23: As in Fig S15 for latent heat flux corrected for surface energy balance closure (positive upward).

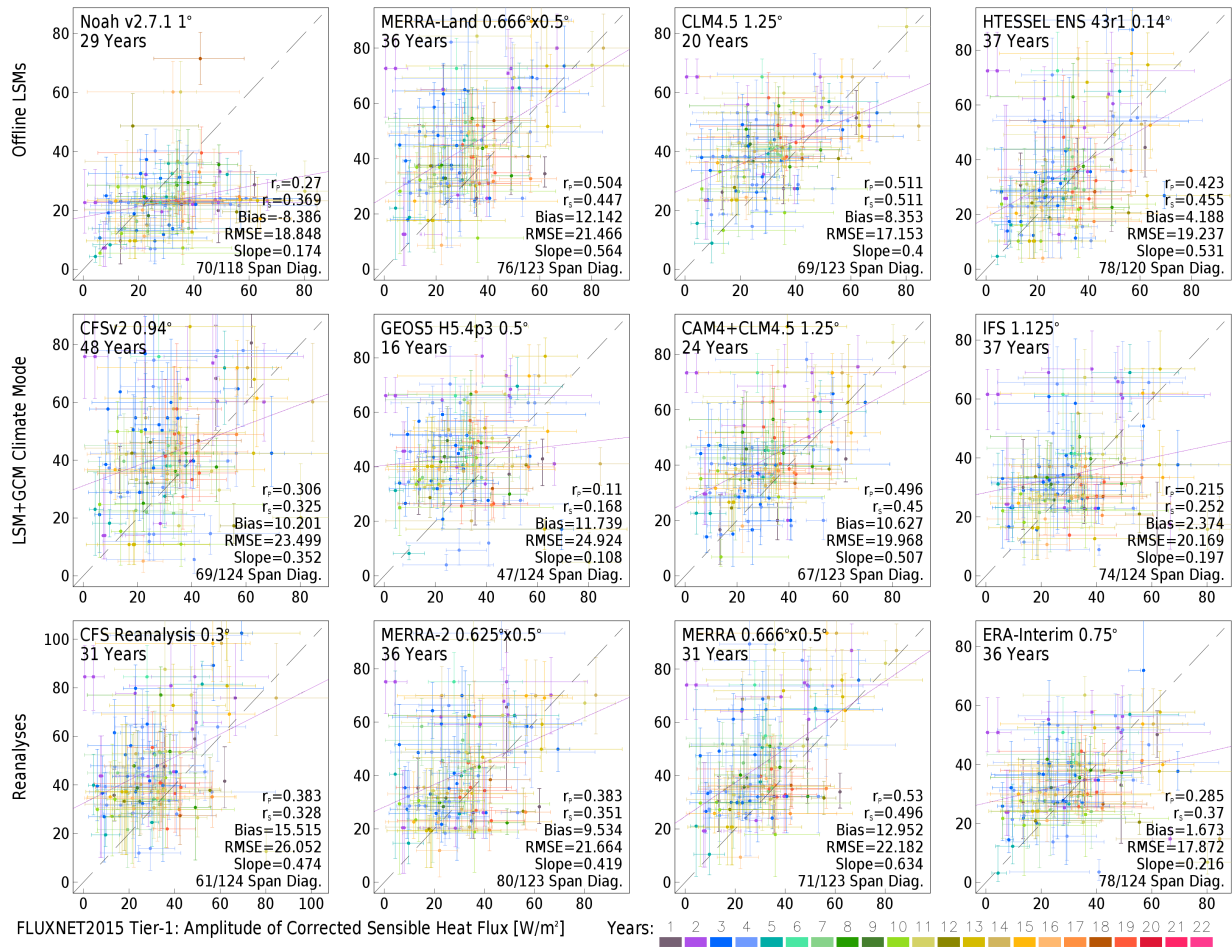


Figure S24: As in Fig S15 for sensible heat flux corrected for surface energy balance closure (positive upward).

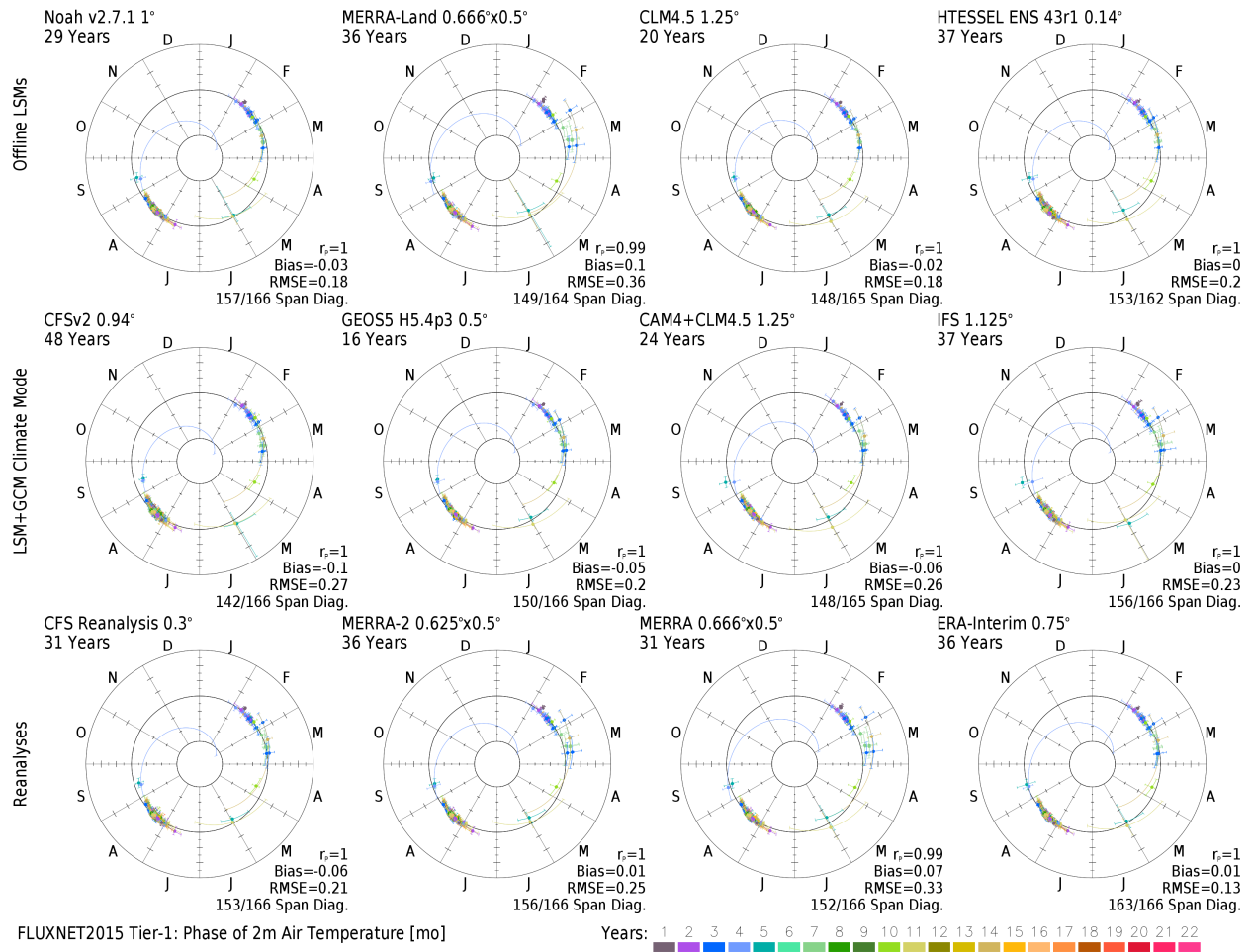


Figure S25: Scatter of the phase of the annual cycle (calculated from the first harmonic of monthly means) of 2m air temperature at FLUXNET2015 sites (azimuth) to multi-decade climatologies (error indicated radially – see below for details); number of years given in upper left of each panel) from offline LSM simulations (top row), coupled LSM+GCM simulations (middle row) or reanalyses constrained by data assimilation (bottom row) using the value from the grid box containing the FLUXNET2015 site location (unless data are missing or indicated to be an all-ocean grid box). Colors indicate years of available data from each FLUXNET2015 site.

The arcing whiskers represent the range of observed FLUXNET2015 phases from individual calendar years, spiraling azimuthally. Model errors are shown radially relative to three concentric circles. The intermediate circle corresponds to zero bias in the phase. Radial displacements inward and outward represent model phasing that is respectively too early or too late, with the innermost and outer circles at minus and plus 6 months in phase error. Radial whiskers indicate the range of phases represented by the models. When either set of whiskers for a point intersect the central concentric circle, the model and observed populations overlap and effectively “span the diagonal” as with Figs 1 and S2-S12.

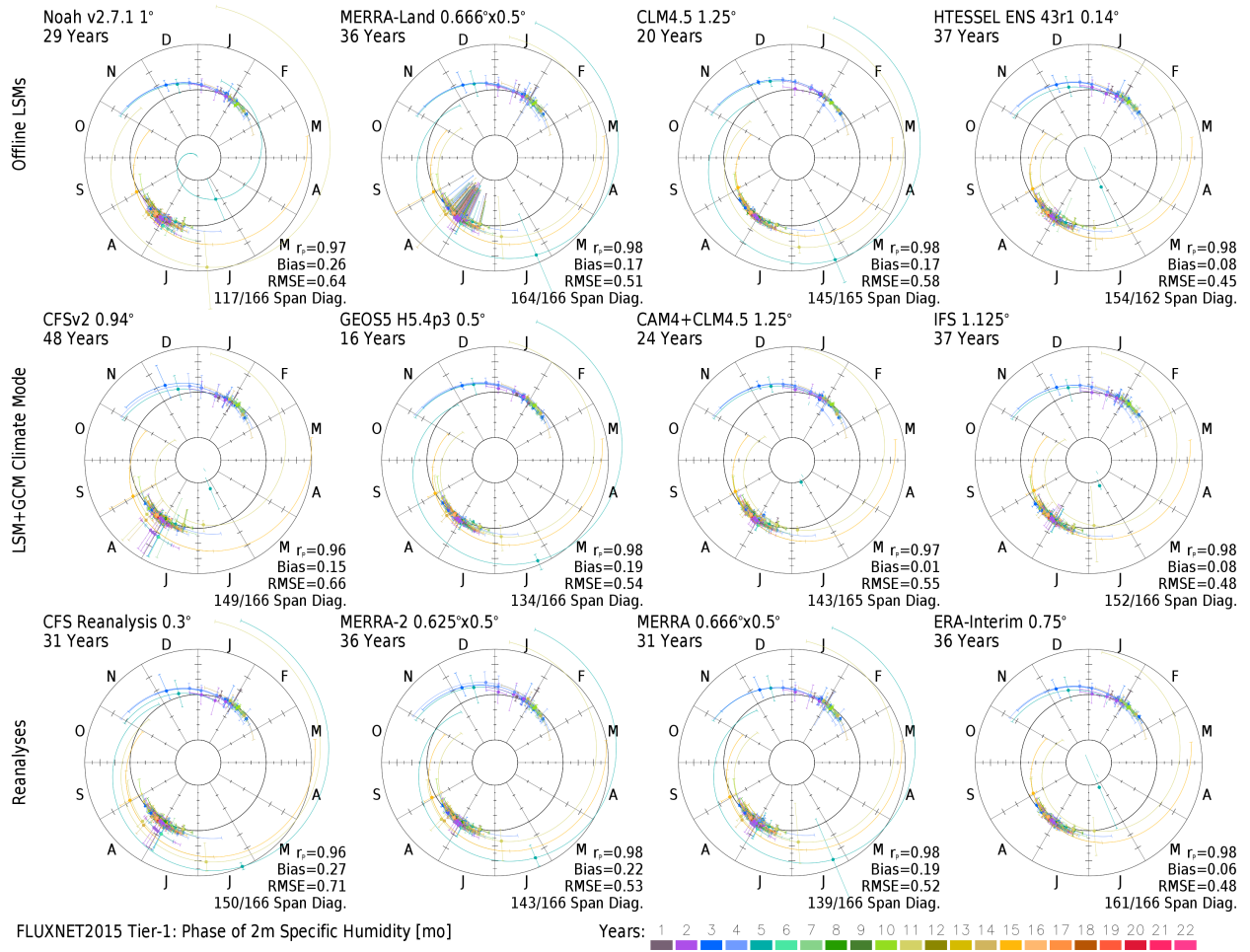


Figure S26: As in S25 for 2m specific humidity.

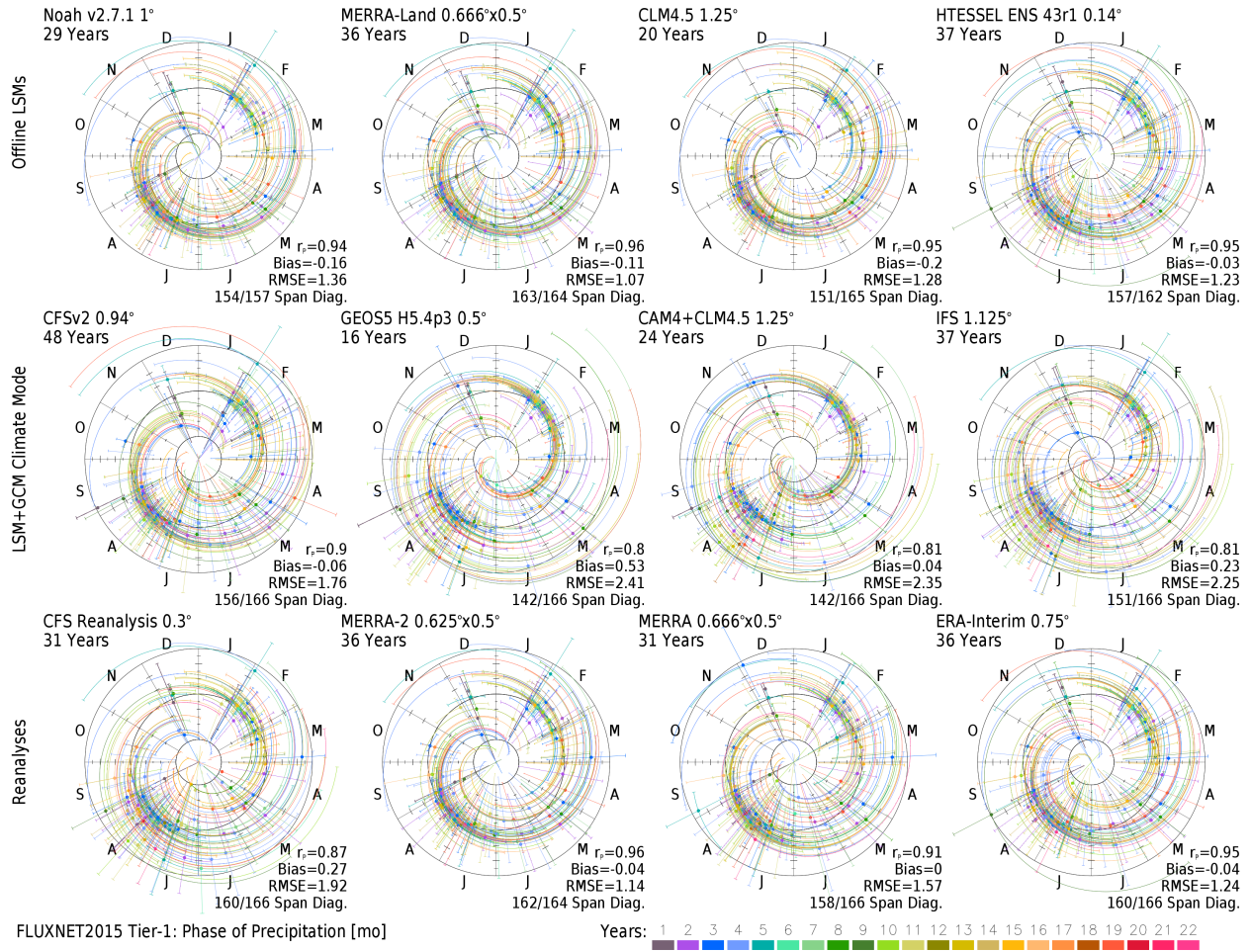


Figure S27: As in S25 for precipitation.

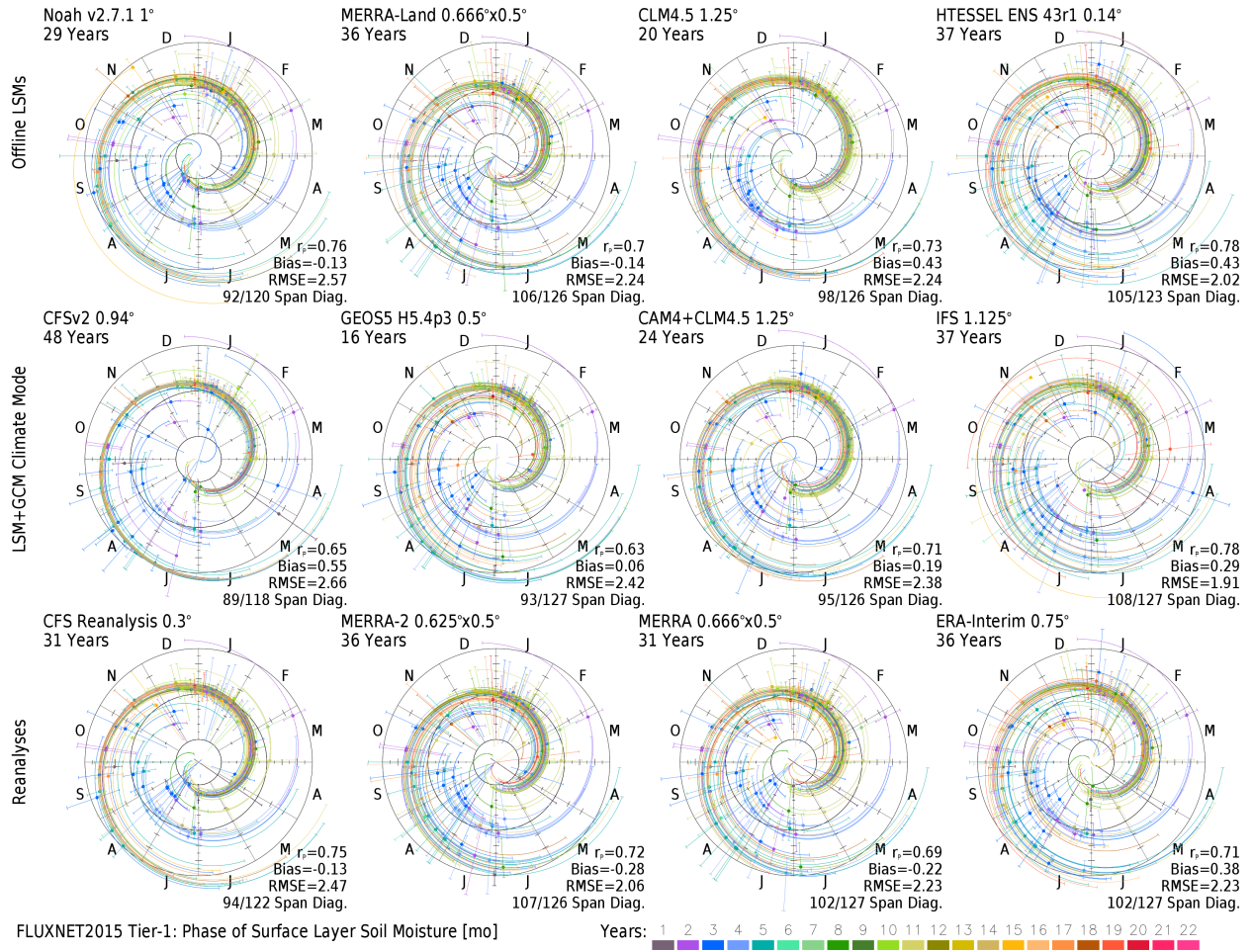


Figure S28: As in S25 for near surface volumetric soil moisture.

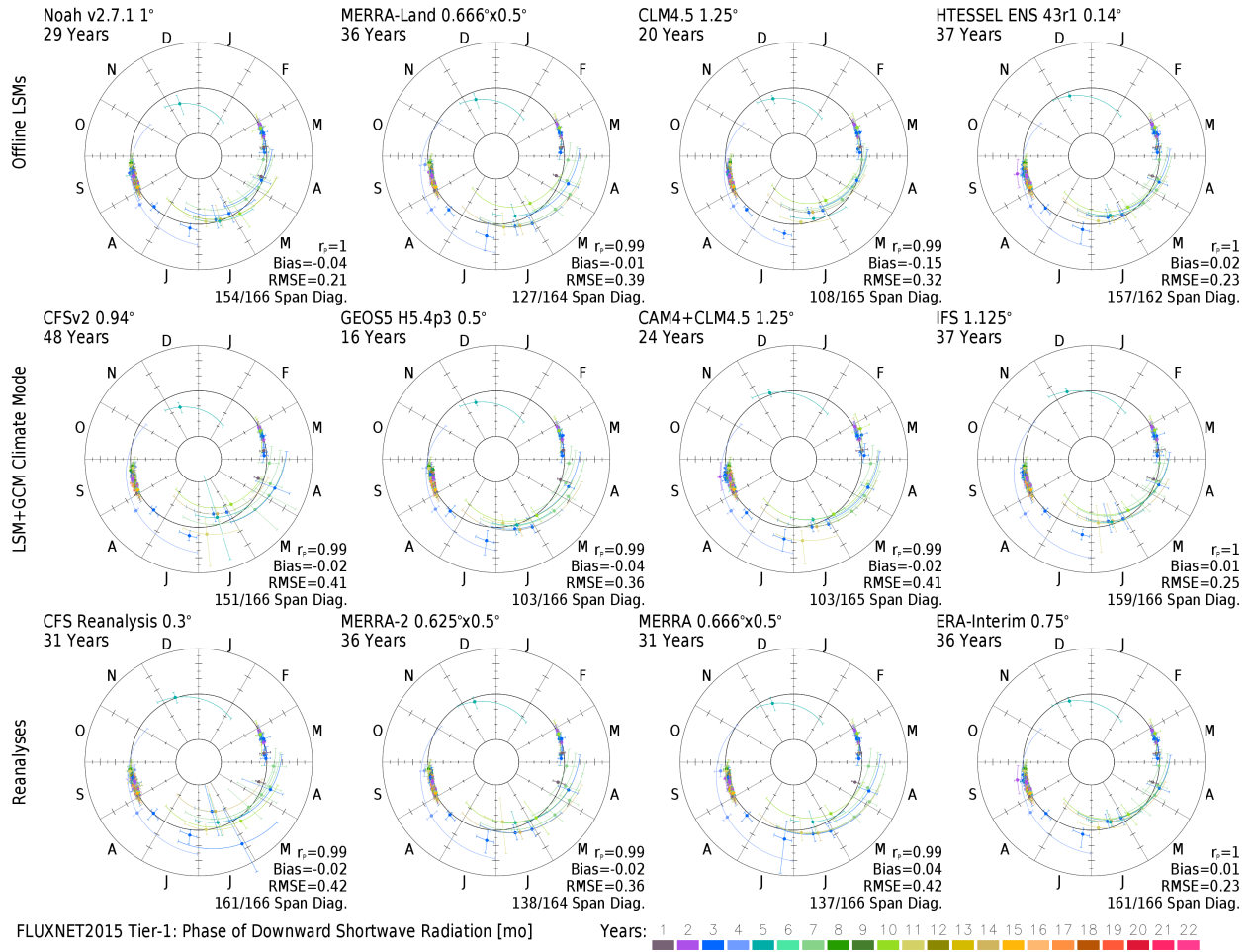


Figure S29: As in S25 for downward shortwave radiation at the surface.

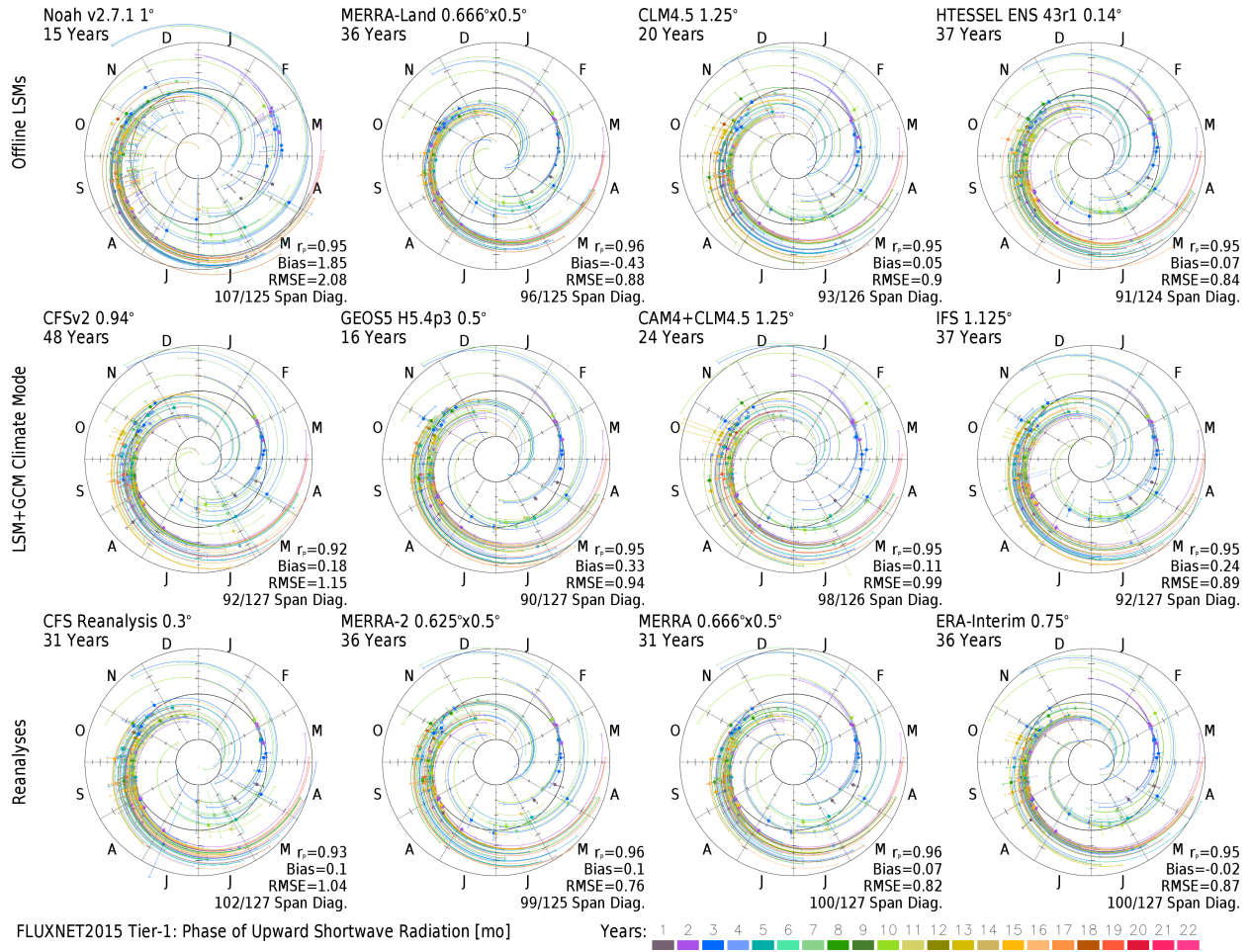


Figure S30: As in S25 for upward shortwave radiation at the surface.

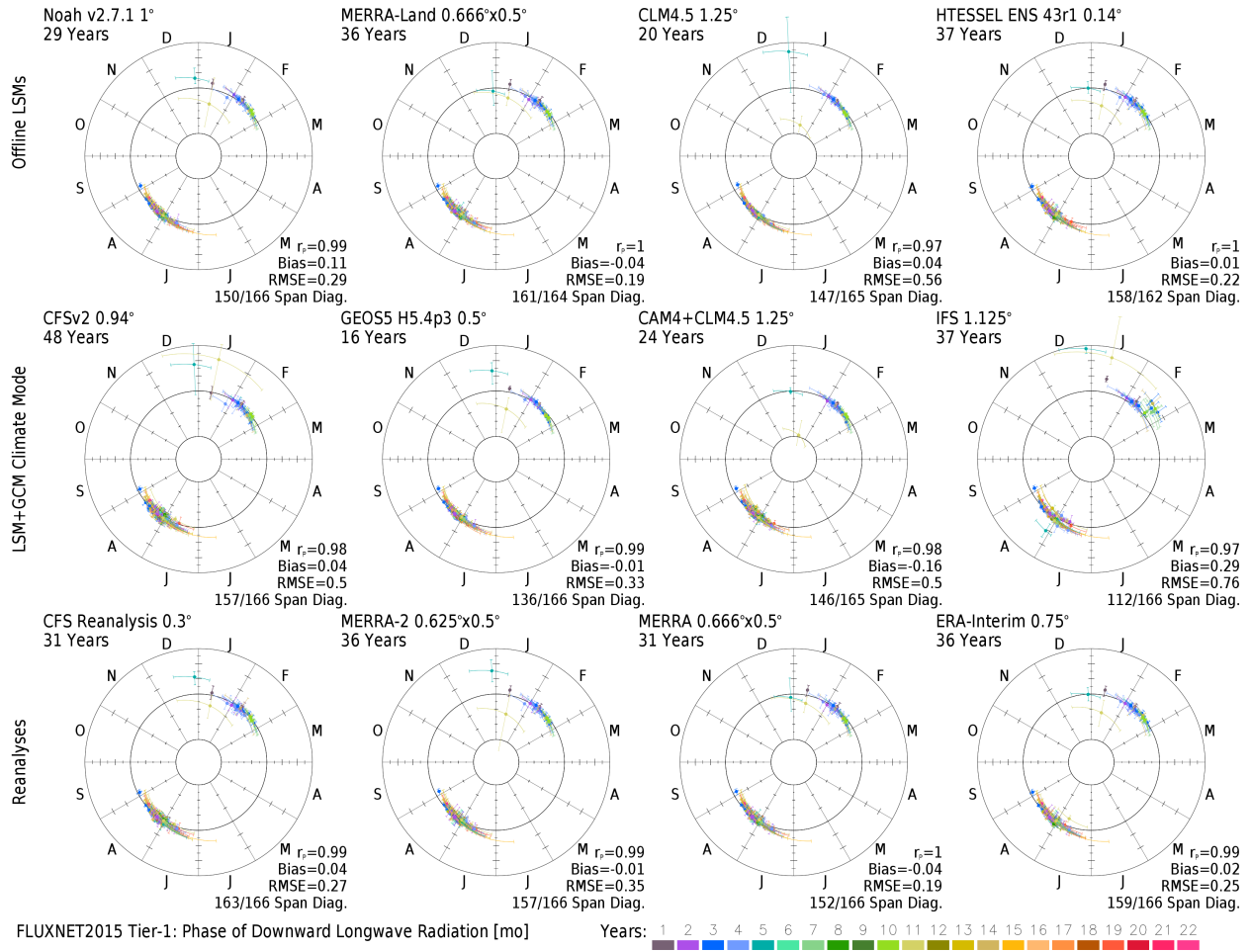


Figure S31: As in S25 for downward longwave radiation at the surface.

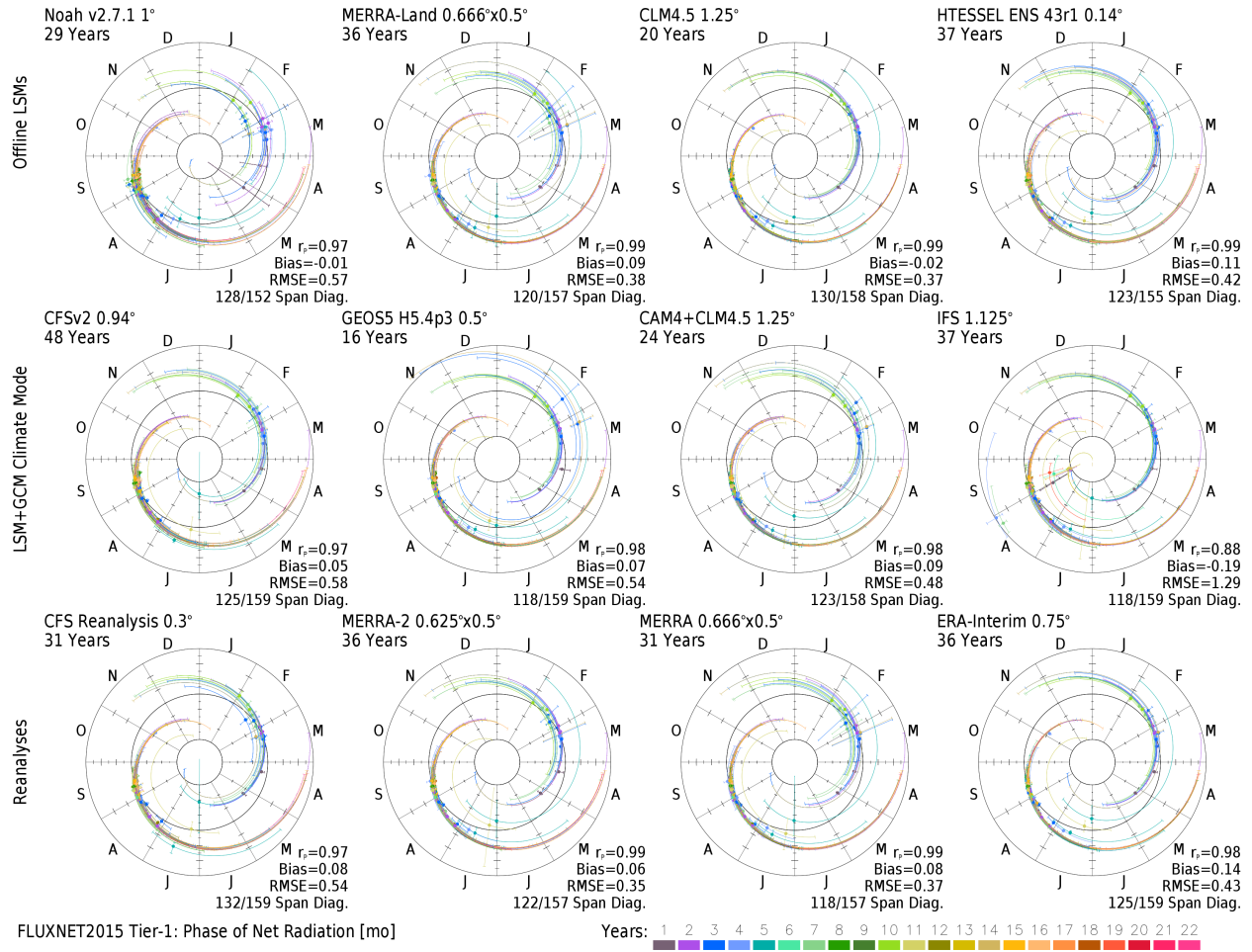


Figure S32: As in S25 for net radiation at the surface (positive downward).

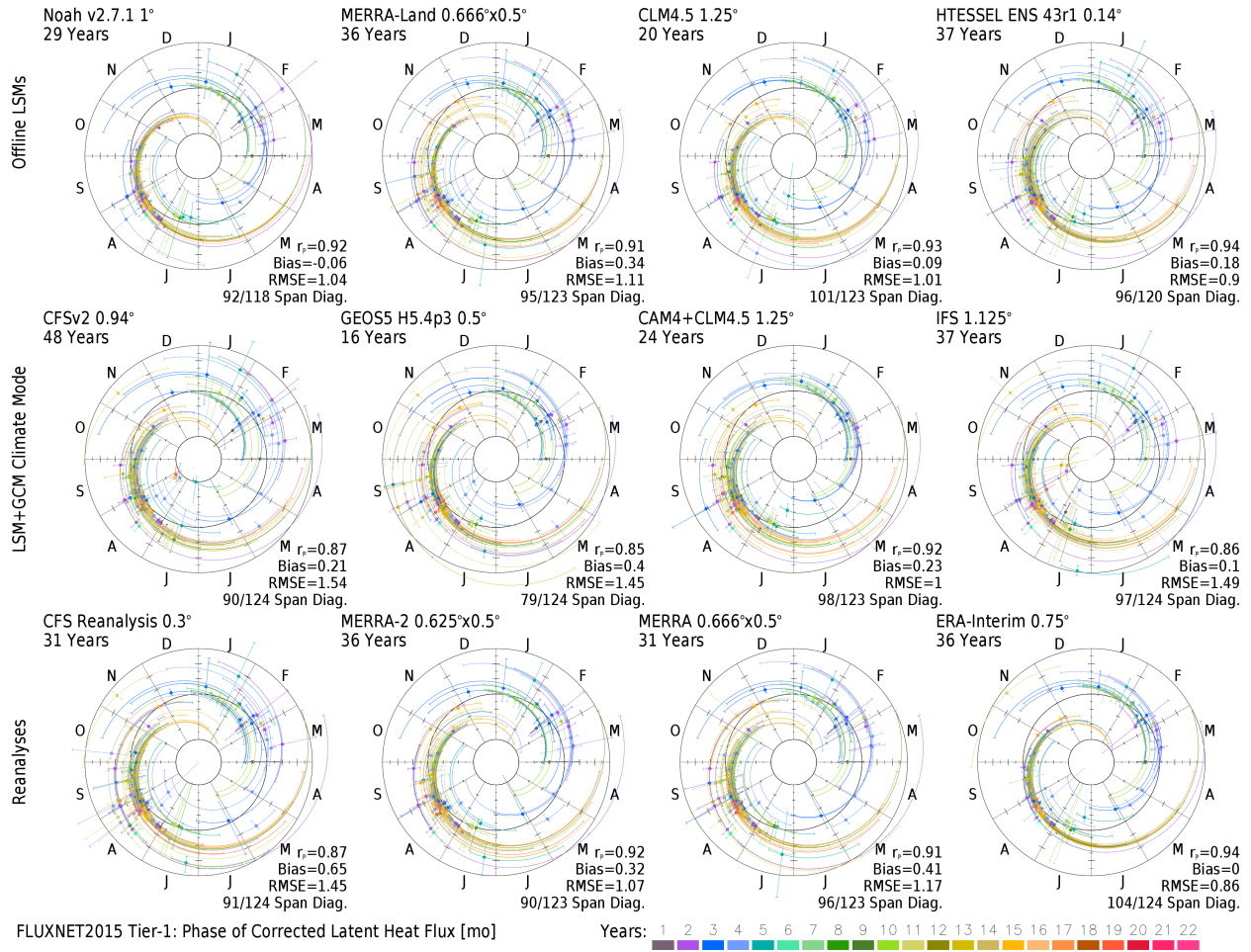


Figure S33: As in S25 for latent heat flux corrected for surface energy balance closure (positive upward).

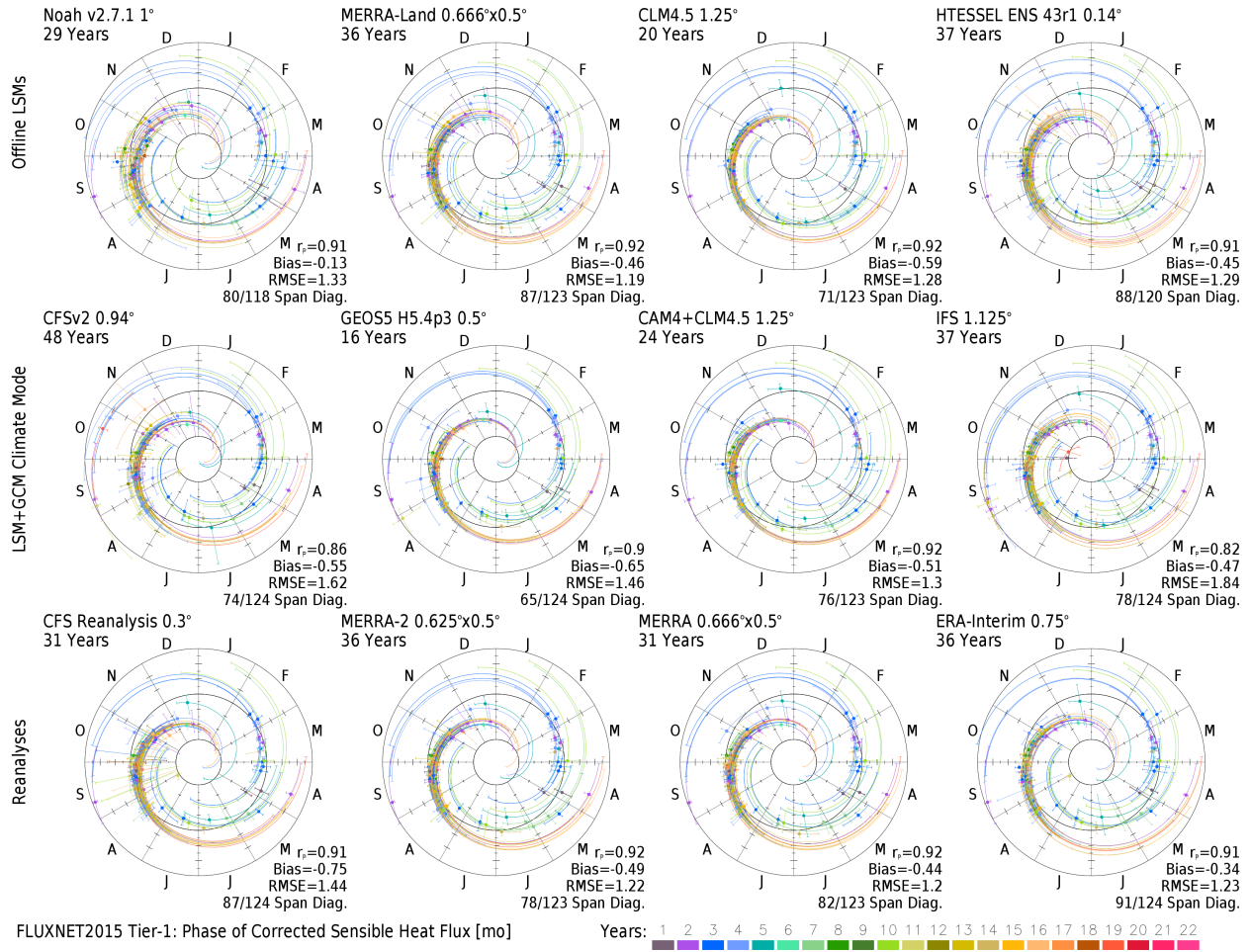


Figure S34: As in S25 for sensible heat flux corrected for surface energy balance closure (positive upward).

References:

- Adler, R. F., G. J. Huffman, A. Chang, R. Ferraro, P. Xie, J. Janowiak, B. Rudolf, U. Schneider, S. Curtis, D. Bolvin, A. Gruber, J. Susskind, and P. Arkin, 2003: The Version 2 Global Precipitation Climatology Project (GPCP) Monthly Precipitation Analysis (1979 - Present). *J. Hydrometeor.*, **4**, 1147-1167.
- Ammann, C., C. R. Flechard, J. Leifeld, A. Neftel, and J. Fuhrer, 2007: The carbon budget of newly established temperate grassland depends on management intensity. *Ag. Ecosys. Env.*, **121**, 5-20, doi: 10.1016/j.agee.2006.12.002.
- Aubinet, M., B. Chermanne, M. Vandenhaute, B. Longdoz, M. Yernaux, and E. Laitat, 2001: Long term carbon dioxide exchange above a mixed forest in the Belgian Ardennes, *Ag. Forest Meteor.*, **108**, 293–315, doi: 10.1016/S0168-1923(01)00244-1.
- Bazot, S., L. Barthes, D. Blanot, and C. Fresneau, 2013: Distribution of non-structural nitrogen and carbohydrate compounds in mature oak trees in a temperate forest at four key phenological stages. *Trees*, **27**, 1023, doi: 10.1007/s00468-013-0853-5.
- Beck, H. E., A. I. J. M. van Dijk, V. Levizzani, J. Schellekens, D. G. Miralles, B. Martens, A. de Roo, 2017: MSWEP: 3-hourly 0.25° global gridded precipitation (1979–2015) by merging gauge, satellite, and reanalysis data. *Hydrol. Earth Sys. Sci.*, **21**, 589-615, doi:10.5194/hess-21-589-2017.
- Belelli Marchesini, L., D. Papale, M. Reichstein, N. Vuichard, N. Tchebakova, and R. Valentini, 2007: Carbon balance assessment of a natural steppe of southern Siberia by multiple constraint approach. *Biogeosci.*, **4**, 581–595, doi: 10.5194/bg-4-581-2007.
- Beringer, J. and Co-authors, 2016: An introduction to the Australian and New Zealand flux tower network – OzFlux. *Biogeosci.*, **13**, 5895-5916, doi: 10.5194/bg-13-5895-2016.
- Bernhofer, C., and Co-authors, 2003: Spruce Forests (Norway and Sitka Spruce, Including Douglas Fir): Carbon and Water Fluxes and Balances, Ecological and Ecophysiological Determinants, in: Fluxes of Carbon, edited by: Valentini, R., Water and Energy of European Forests, Springer-Verlag, Berlin.
- Bonal, D., and Co-authors, 2008: Impact of severe dry season on net ecosystem exchange in the Neotropical rainforest of French Guiana. *Glob. Change Biol.*, **14**, 1917-1933, doi: 10.1111/j.1365-2486.2008.01610.x.
- Borchard, N., M. Schirrmann, C. von Hebel, M. Schmidt, R. Baatz, L. Firbank, H. Vereecken, and M. Herbst, 2015: Spatio-temporal drivers of soil and ecosystem carbon fluxes at field scale in an upland grassland in Germany. *Ag. Ecosys. Env.*, **211**, 84-93, doi: 10.1016/j.agee.2015.05.008.
- Dařenova, E., T. Fabianek, and M. Pavelka, 2016: Effect of repeated spring drought and summer heavy rain on managed grassland biomass production and CO₂ efflux. *Eur. J. Env. Sci.*, **6**, 98-102, doi: 10.14712/23361964.2016.14.

- Dařenova, E., P. Holub, L. Krupkova, and M. Pavelka, 2017: Efflux of CO₂ from soil in Norway spruce stands of different ages: A case study. *Eur. J. Env. Sci.*, **6**, 98-102, doi: 10.14712/23361964.2016.14.
- Dietiker, D., N. Buchmann, and W. Eugster, 2010: Testing the ability of the DNDC model to predict CO₂ and water vapour fluxes of a Swiss cropland site. *Ag. Ecosys. Env.*, **139**, 396-401, doi: 10.1016/j.agee.2010.09.002.
- Fest, B. J., N. Hinko-Najera, T. Wardlaw, D. W. T. Griffith, S. J. Livesley, and S. K. Arndt, 2017: Soil methane oxidation in both dry and wet temperate eucalypt forests shows a near-identical relationship with soil air-filled porosity. *Biogeosci.*, **14**, 467-479, doi: 10.5194/bg-14-467-2017.
- Galvagno, M., and Co-authors, 2013: Phenology and carbon dioxide source/sink strength of a subalpine grassland in response to an exceptionally short snow season. *Environ. Res. Lett.*, **8**, 25008, doi: 10.1088/1748-9326/8/2/025008.
- Gash, J. H. C. and A. J. Dolman, 2003: Sonic anemometer (co)sine response and flux measurement I. The potential for (co)sine error to affect sonic anemometer-based flux measurements. *Ag. Forest Meteor.*, **119**, 195–207, doi: 10.1016/S0168-1923(03)00137-0.
- Gilmanov, T. G., and Co-authors, 2007: Partitioning European grassland net ecosystem CO₂ exchange into gross primary productivity and ecosystem respiration using light response function analysis. *Ag. Ecosys. Environ.*, **121**, 93–120, doi: 10.1016/j.agee.2006.12.008.
- Heim, A., L. Wehrli, W. Eugster, and M. W. I. Schmidt, 2008: Effects of sampling design on the probability to detect soil carbon stock changes at the Swiss CarboEurope site Lägeren. *Geoderma*, **149**, 347-354, doi: 10.1016/j.geoderma.2008.12.018.
- Huffman, G. J., R. F. Adler, M. M. Morrissey, S. Curtis, R. Joyce, B. McGavock, and J. Susskind, 2001: Global precipitation at one-degree daily resolution from multi-satellite observations. *J. Hydrometeor.*, **2**, 36-50.
- Huffman, G. J., R. F. Adler, D. T. Bolvin, G. Gu, E. J. Nelkin, K. P. Bowman, Y. Hong, E. F. Stocker, and D. B. Wolff, 2007: The TRMM Multi-satellite Precipitation Analysis: Quasi-Global, Multi-Year, Combined-Sensor Precipitation Estimates at Fine Scale. *J. Hydrometeor.*, **8**, 38-55.
- Imer, D., L. Merbold, W. Eugster, and N. Buchmann, 2013: Temporal and spatial variations of soil CO₂, CH₄ and N₂O fluxes at three differently managed grasslands. *Biogeosci.*, **10**, 5931–5945, doi: 10.5194/bg-10-5931-2013.
- Jamali, H., S. J. Livesley, T. Z. Dawes, G. D. Cook, L. B. Hutley, and S. K. Arndt, 2011: Diurnal and seasonal variations in CH₄ flux from termite mounds in tropical savannas of the Northern Territory, Australia. *Ag. Forest Meteor.*, **151**, 1471–1479, doi: 10.1016/j.agrformet.2010.06.009.

- Jung, M., M. Reichstein, and A. Bondeau, 2009: Towards global empirical upscaling of FLUXNET eddy covariance observations: validation of a model tree ensemble approach using a biosphere model, *Biogeosci.*, **6**, 2001–2013, doi: 10.5194/bg-6-2001-2009.
- King, M. D., S. Platnick, C. C. Moeller, H. E. Revercomb, and D. A. Chu, 2003: Remote sensing of smoke, land, and clouds from the NASA ER-2 during SAFARI 2000. *J. Geophys. Res.*, **108**, 8502, doi: 10.1029/2002JD003207.
- Knohl, A., E.-D. Schulze, O. Kolle, and N. Buchmann, 2003: Large carbon uptake by an unmanaged 250-year-old deciduous forest in Central Germany. *Ag. Forest Meteor.*, **118**, 151–167, doi: 10.1016/S0168-1923(03)00115-1.
- Li, X., and Co-authors, 2013: Estimation of gross primary production over the terrestrial ecosystems in China. *Ecol. Model.*, **261–262**, 80–92, doi: 10.1016/j.ecolmodel.2013.03.024.
- Loubet, B., and Co-authors, 2011: Carbon, nitrogen and greenhouse gases budgets over a four years crop rotation in northern France. *Plant Soil*, **343**, 109–137, doi: 10.1007/s11104-011-0751-9.
- Lund, M., J. M. Falk, T. Friberg, H. N. Mbufong, C. Sigsgaard, H. Soegaard, and M. P. Tamstorf, 2012: Trends in CO₂ exchange in a high Arctic tundra heath, 2000–2010. *J. Geophys. Res.*, **117**, G02001, doi: 10.1029/2011JG001901.
- Matsuura, K., and C. J. Willmott. 2014. Terrestrial precipitation: 1900–2014 gridded monthly time series (Version 4.01). Newark: Center for Climatic Research, Department of Geography, University of Delaware. <http://climate.geog.udel.edu/~climate/> (last accessed 29 August 2016).
- Merbold, L., W. L. Kutsch, C. Corradi, O. Kolle, C. Rebmann, P. C. Stoy, S. A. Zimov, and E.-D. Schulze, 2009: Artificial drainage and associated carbon fluxes (CO₂/CH₄) in a tundra ecosystem. *Glob. Change Biol.*, **15**, 2599–2614, doi: 10.1111/j.1365-2486.2009.01962.x.
- Merbold, L., W. Eugster, J. Stieger, M. Zahniser, D. Nelson, and N. Buchmann, 2014: Greenhouse gas budget (CO₂, CH₄ and N₂O) of intensively managed grassland following restoration. *Glob. Change Biol.*, **20**, 1913–1928, doi: 10.1111/gcb.12518.
- Moureaux, C., A. Debacq, B. Bodson, B. Heinesch, and M. Aubinet, 2006: Annual net ecosystem carbon exchange by a sugar beet crop. *Ag. Forest Meteor.*, **139**, 25–39, doi: 10.1016/j.agrformet.2006.05.009.
- Rambal, S., R. Joffre, J. M. Ourcival, J. Cavender-Bares, and A. Rocheteau, A., 2004: The growth respiration component in eddy CO₂ flux from a Quercus ilex mediterranean forest, *Glob. Change Biol.*, **10**, 1460–1469, doi: 10.1111/j.1365-2486.2004.00819.x.
- Reichstein, M., and Co-authors, 2003: Modeling temporal and large-scale spatial variability of soil respiration from soil water availability, temperature and vegetation productivity indices. *Glob. Biogeochem. Cycles*, **17**, 1104, doi: 10.1029/2003GB002035.

- Reichstein, M., and Co-authors, 2005: On the separation of net ecosystem exchange into assimilation and ecosystem respiration: review and improved algorithm. *Glob. Change Biol.*, **11**, 1424–1439, doi: 10.1111/j.1365-2486.2005.001002.x.
- Revill, A., O. Sus, B. Barrett, and M. Williams, 2013: Carbon cycling of European croplands: A framework for the assimilation of optical and microwave Earth observation data. *Remote Sens. Environ.*, **137**, 84–93, doi: 10.1016/j.rse.2013.06.002.
- Rey, A., E. Pegoraro, V. Tedeschi, I. De Parri, P. G. Jarvis, and R. Valentini, 2002: Annual variation in soil respiration and its components in a coppice oak forest in Central Italy. *Glob. Change Boil.*, **8**, 851-866, doi: 10.1046/j.1365-2486.2002.00521.x.
- Schmidt, M., T. G. Reichenau, P. Fiener, and K. Schneider, 2012: The carbon budget of a winter wheat field: An eddy covariance analysis of seasonal and inter-annual variability. *Ag. Forest Meteor.*, **165**, 114-126, 10.1016/j.agrformet.2012.05.012.
- Sjöström, M., J. Ardö, L. Eklundh, B. A. El-Tahir, H. A. M. El-Khidir, M. Hellström, P. Pilesjö, and J. Seaquist, 2009: Evaluation of satellite based indices for gross primary production estimates in a sparse savanna in the Sudan. *Biogeosci.*, **6**, 129-138, doi: 10.5194/bg-6-129-2009.
- Soegaard, H. and C. Nordstroem, 1999: Carbon dioxide exchange in a high-arctic fen estimated by eddy covariance measurements and modelling. *Glob. Change Biol.*, **5**, 547–562, doi: 10.1111/j.1365-2486.1999.00250.x.
- Stoy, P. C., and Co-authors, 2011: A data-driven analysis of energy balance closure across FLUXNET research sites: The role of landscape scale heterogeneity. *Ag. Forest Meteor.*, **171–172**, 137–152, doi: 10.1016/j.agrformet.2012.11.004.
- Sulkava, M., S. Luyssaert, S. Zaehle, and D. Papale, 2011: Assessing and improving the representativeness of monitoring networks: The European flux tower network example. *J. Geophys. Res.*, **116**, G00J04, doi: 10.1029/2010JG001562.
- Suni, T., J. Rinne, A. Reissell, N. Altimir, P. Keronen, U. Rannik, M. DalMaso, M. Kulmala, and T. Vesala, 2003: Long-term measurements of surface fluxes above a Scots pine forest in Hyytiala, southern Finland. 1996–2001, *Boreal Environ. Res.*, **8**, 287–301.
- Tagesson, T., R. Fensholt, F. Cropley, I. Guiro, S. Horion, A. Ehammer, and J. Ardö, 2015: Dynamics in carbon exchange fluxes for a grazed semi-arid savanna ecosystem in West Africa. *Ag. Ecosyst. Env.*, **205**, 15-24, doi: 10.1016/j.agee.2015.02.017.
- Tedeschi, V., A. Rey, G. Manca, R. Valentini, P. G. Jarvis, and M. Borghetti, 2006: Soil respiration in a Mediterranean oak forest at different developmental stages after coppicing. *Glob. Change Biol.*, **12**, 110–121, doi: 10.1111/j.1365-2486.2005.01081.x.
- Viovy, N., 2013. CRUNCEP data set for 1901–2010, [Available at <https://vesg.ipsl.upmc.fr/thredds/fileServer/store/p529viov/cruncep/readme.html>].
- Weedon, G. P., and co-authors, 2011: Creation of the WATCH forcing data and its use to assess global and regional reference crop evaporation over land during the Twentieth Century. *J. Hydrometeor.*, **12**, 823-848, doi: 10.1175/2011JHM1369.1.

- Wei, S., and Co-authors, 2014: Data-based perfect-deficit approach to understanding climate extremes and forest carbon assimilation capacity. *Environ. Res. Lett.*, **9**, 65002, doi: 10.1088/1748-9326/9/6/065002.
- Westergaard-Nielsen, A., M. Lund, B. U. Hansen, and M. P. Tamsdorf, 2013: Camera derived vegetation greenness index as proxy for gross primary production in a low Arctic wetland area. *ISPRS J. Photogram. Remote Sens.*, **86**, 89-99, doi: 10.1016/j.isprsjprs.2013.09.006.
- Xie, P., A. Yatagai, M. Chen, T. Hayasaka, Y. Fukushima, C. Liu, and S. Yang, 2007: A gauge-based analysis of daily precipitation over East Asia, *J. Hydrometeor.*, **8**, 607-626.
- Zeller, K. and T. Hehn, 1996: Measurements of upward turbulent ozone fluxes above a subalpine spruce-fir forest. *Geophys. Res. Lett.*, **23**, 841–844, doi: 10.1029/96GL00786.